Measurement of the W-boson mass with the ATLAS detector

N. Andari
(University of Birmingham)

LLR Palaiseau
February 13, 2017

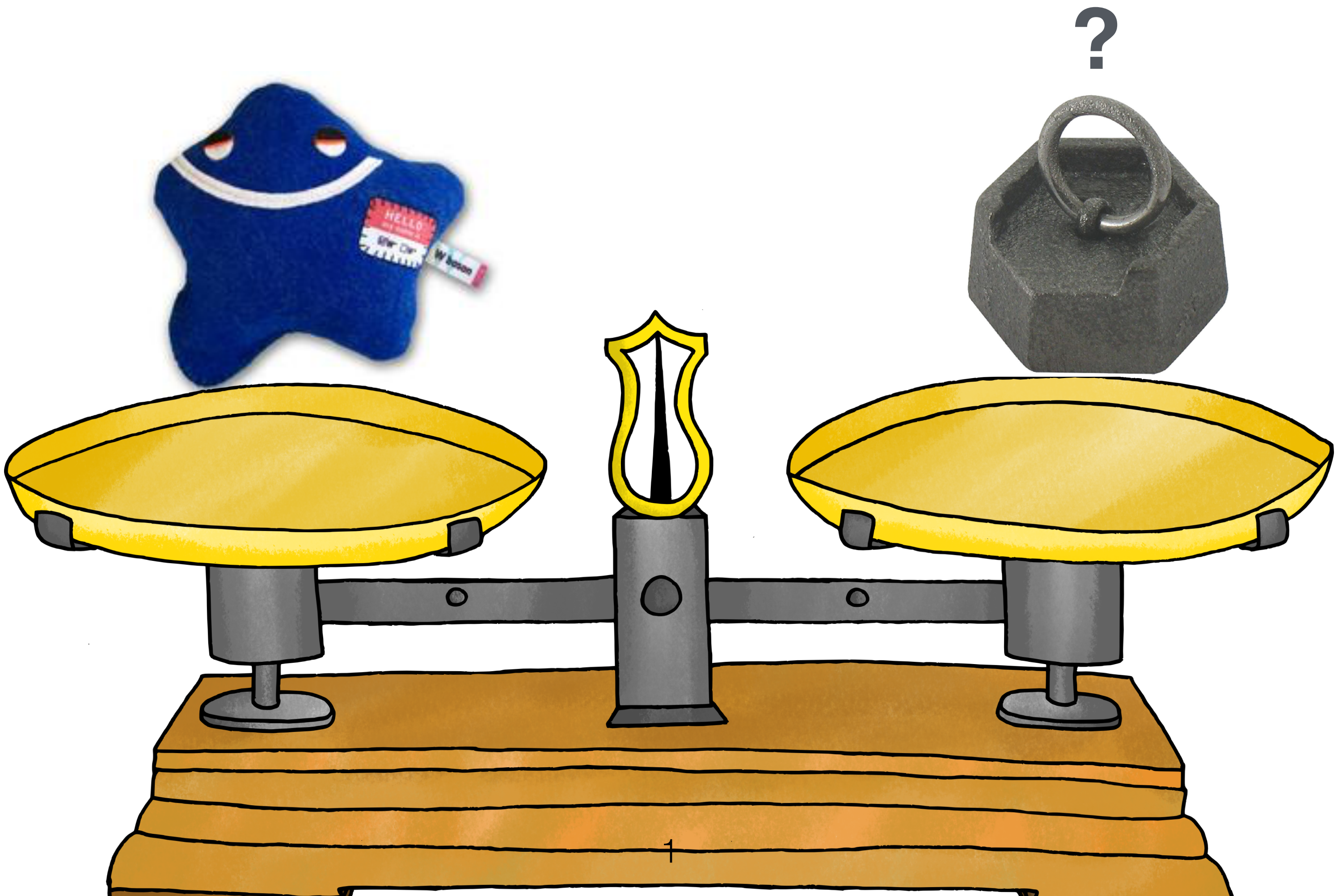

Motivation of the measurement

In the electroweak sector of the SM, the W mass is defined by:

In the on-shell scheme: $$m_W^2\left(1-\frac{m_W^2}{m_Z^2}\right)=\frac{\pi\alpha}{\sqrt{2}G_F}(1+\Delta r)$$

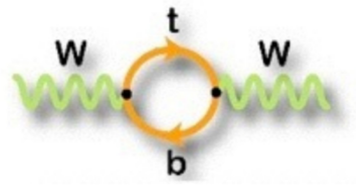

Δr reflects loop corrections and depends on m_t^2 and $\ln m_H$

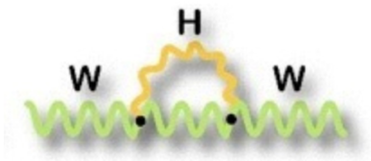

The relation between M_W, m_t, and M_H provides stringent test of the SM and is sensitive to new Physics

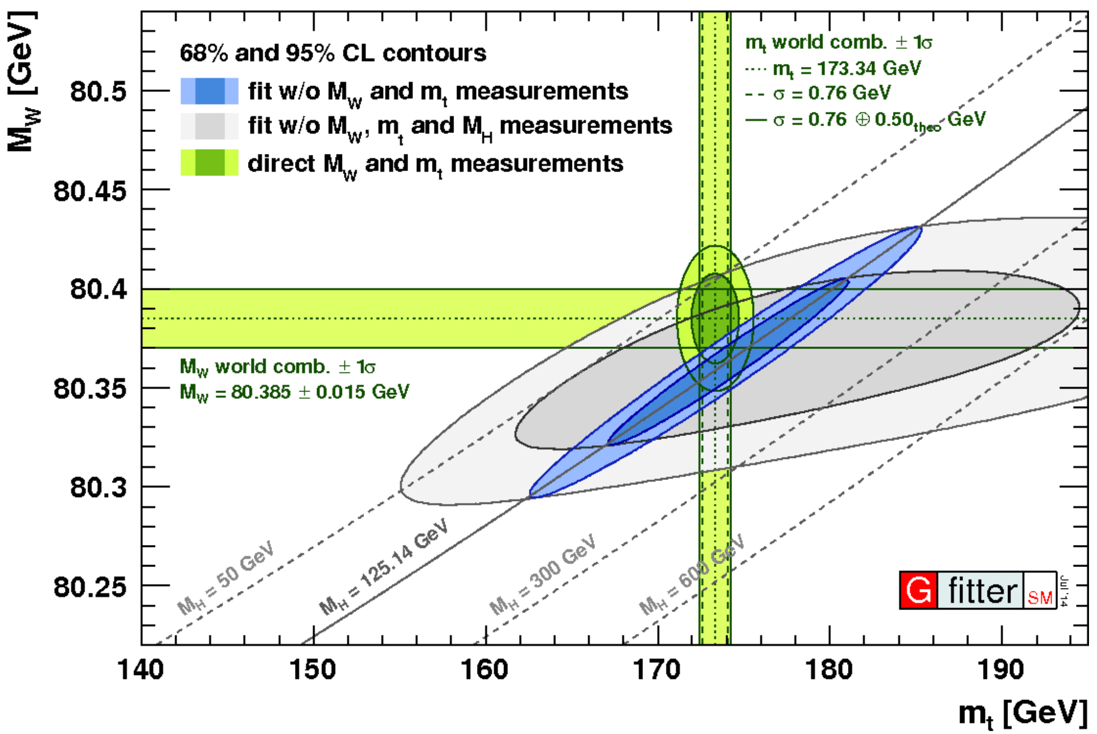

Status of the measurements

Higgs mass

[Phys. Rev. Lett. 114, 191803]

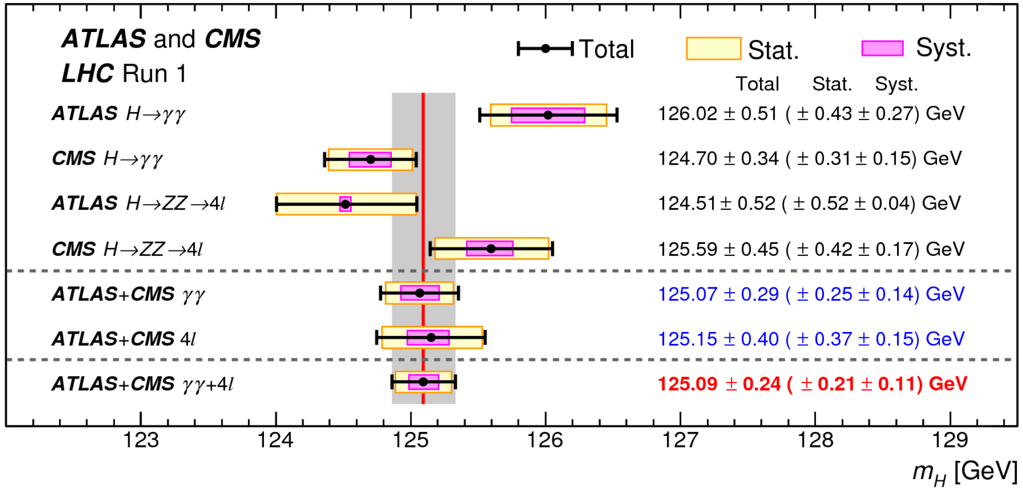

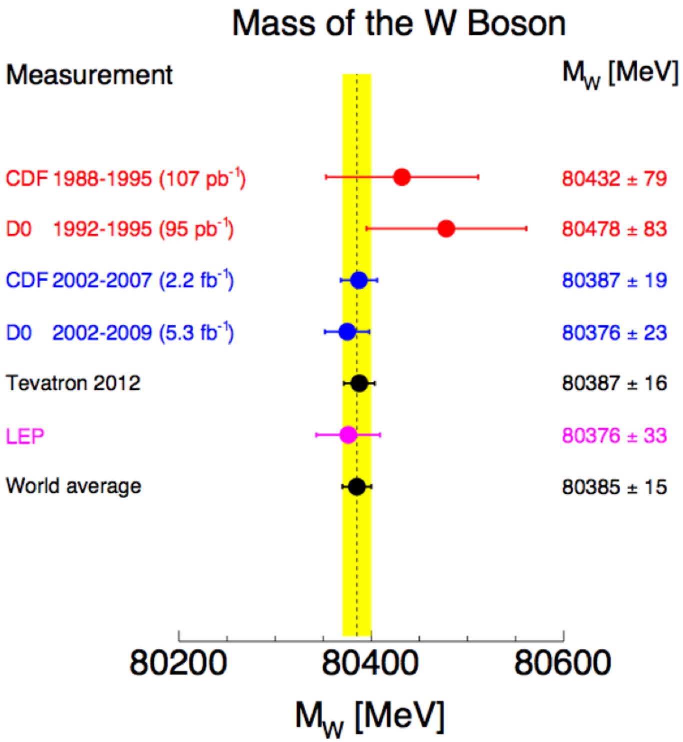

Top mass

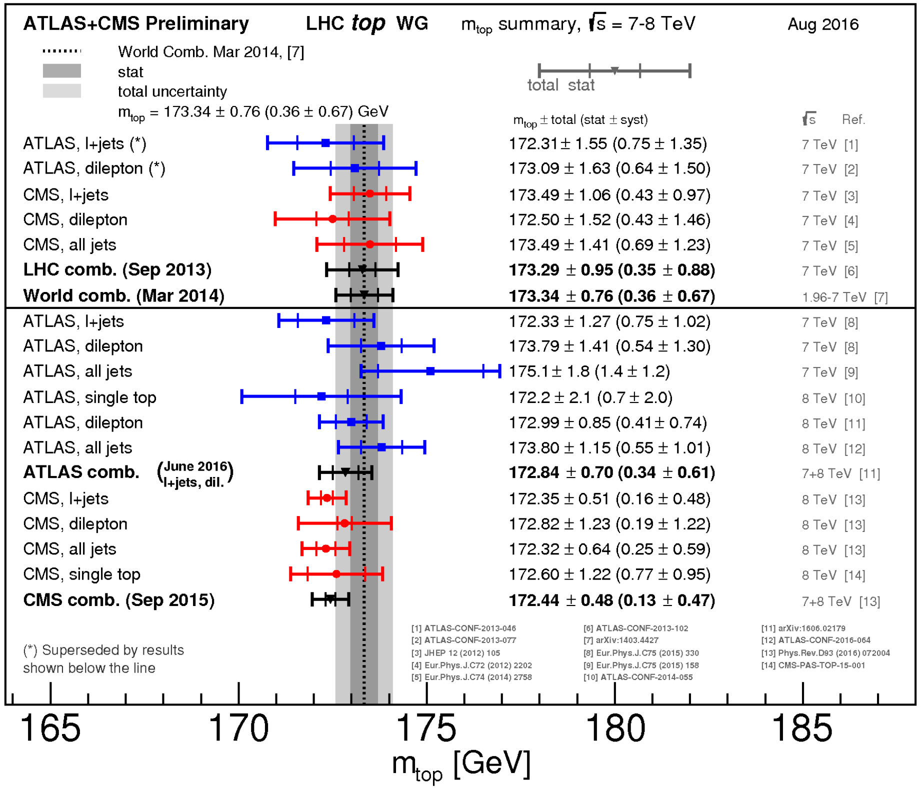

W mass

World average uncertainty ~15 MeV

Best individual measurement: CDF 19 MeV

Tevatron results

CDF experiment:

[Phys. Rev. Lett.108 (2012) 151803]

electron/muon channels
2.2 fb^{-1} integrated luminosity

m_W= 80387+/12(stat)+/-15(syst) MeV

Source	Uncertainty (MeV)
Lepton energy scale and resolution	7
Recoil energy scale and resolution	6
Lepton removal	2
Backgrounds	3
$p_T(W)$ model	5
Parton distributions	10
QED radiation	4
W-boson statistics	12
Total	19

D0 experiment:

[Phys. Rev. Lett. 108 (2012) 151804]

electron channel
4.3 fb^{-1} integrated luminosity

m_W= 80375+/11(stat)+/-20(syst) MeV

	ΔM_W (MeV)		
Source	m_T	p_T^e	$\not{E}_T$
Electron energy calibration	16	17	16
Electron resolution model	2	2	3
Electron shower modeling	4	6	7
Electron energy loss model	4	4	4
Hadronic recoil model	5	6	14
Electron efficiencies	1	3	5
Backgrounds	2	2	2
Experimental subtotal	18	20	24
PDF	11	11	14
QED	7	7	9
Boson p_T	2	5	2
Production subtotal	13	14	17
Total	22	24	29

$$M_W = 80\,387 \pm 16 \text{ MeV}$$

Tevatron vs LHC

proton-antiprotons collisions $\sqrt{s}$=1.96 TeV

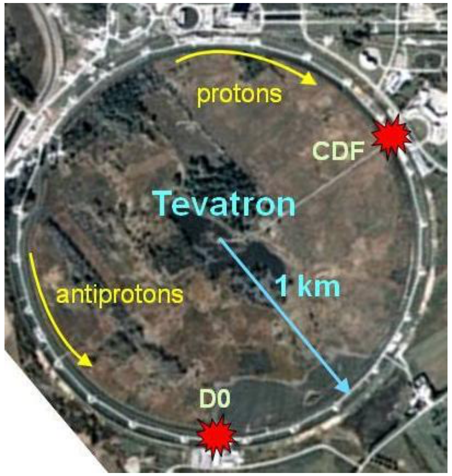

proton-protons collisions $\sqrt{s}$=7 TeV

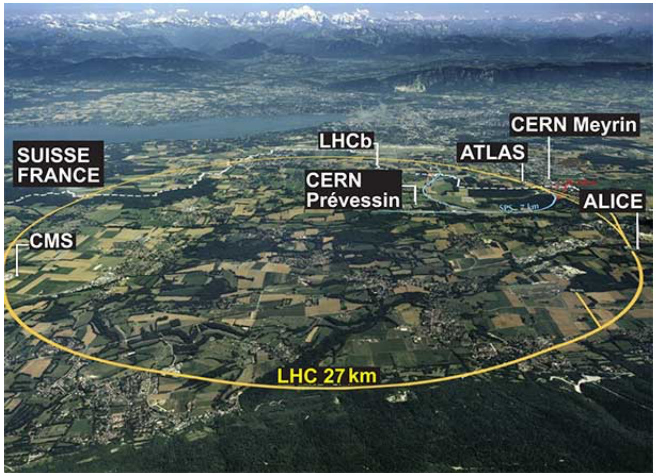

@LHC: Even more challenging and difficult to perform the measurement

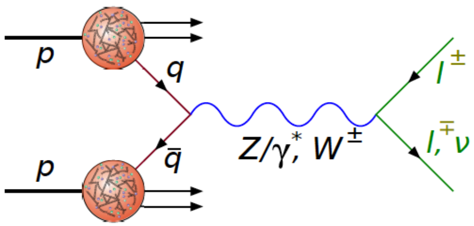

- higher pile-up environment: difficult hadronic recoil calibration, worse resolution
- W^+/W^- production is asymmetric —> charge-dependent analysis
- The sea-quark PDFs play a larger role at the LHC *(25% of the W-boson production is induced by at least one second generation quark s or c).*
- The valence-sea difference as well as the amount of sea quarks with u and d

Valence vs sea quarks

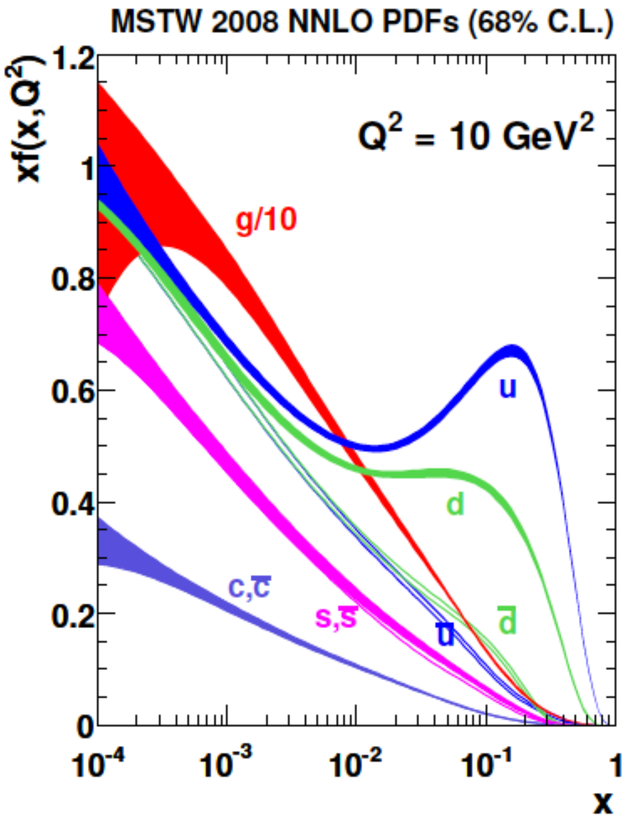

arXiv:1004.2597

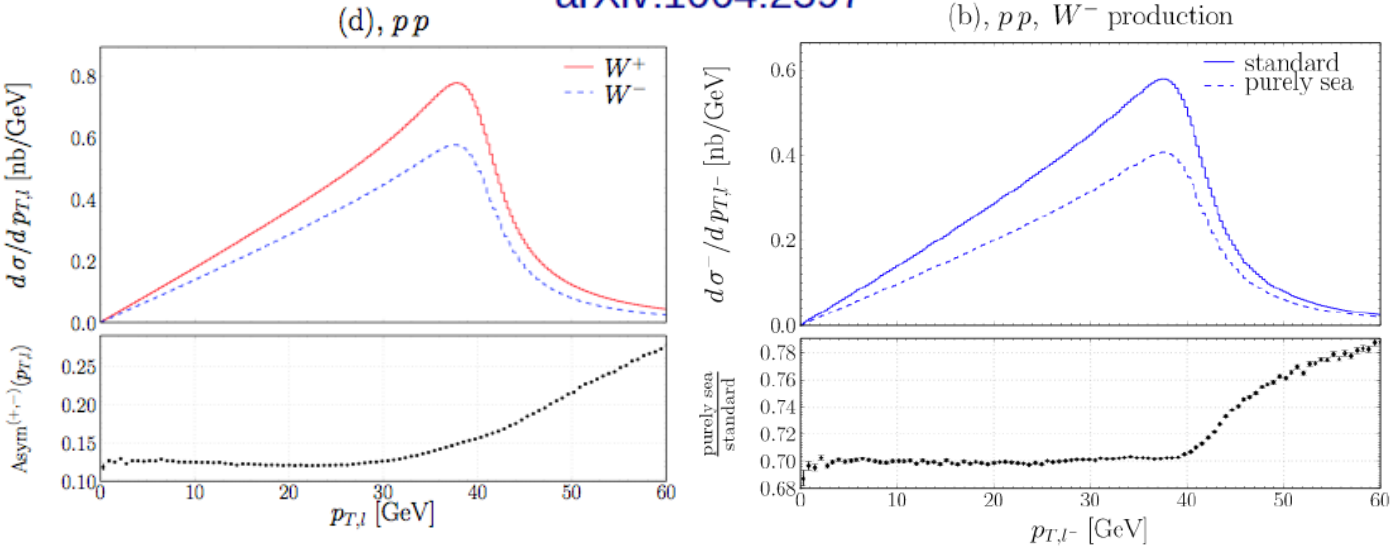

The uncertainty in u and d valence and sea PDF —> an uncertainty in helicity axis of the W —> on p_T^l spectrum

ATL-PHYS-PUB-2014-015

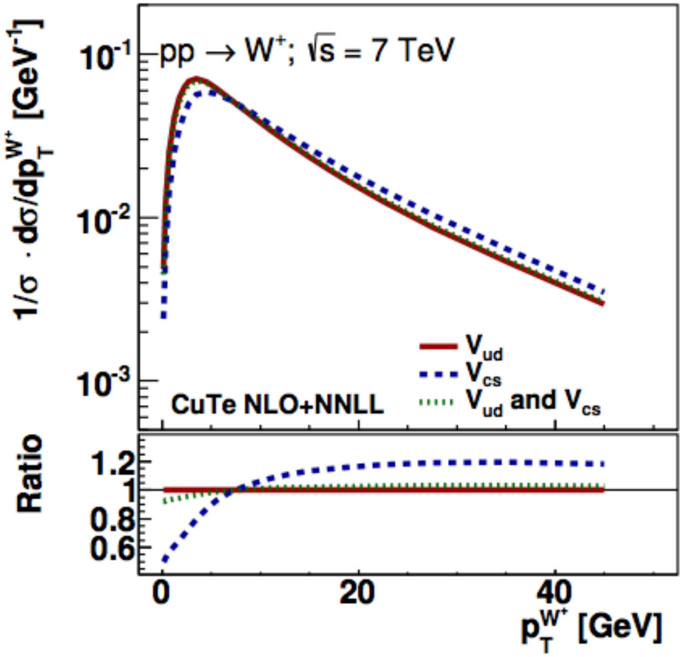

Strange quark pdf uncertainty —> uncertainty on the relative fraction of charm-initiated W boson production —> uncertainty on $p_T(W)$

The amount of charm initiated W production will also alter the balance between valence quark and sea quark —> W polarisation —> p_T^l

Despite the challenge!

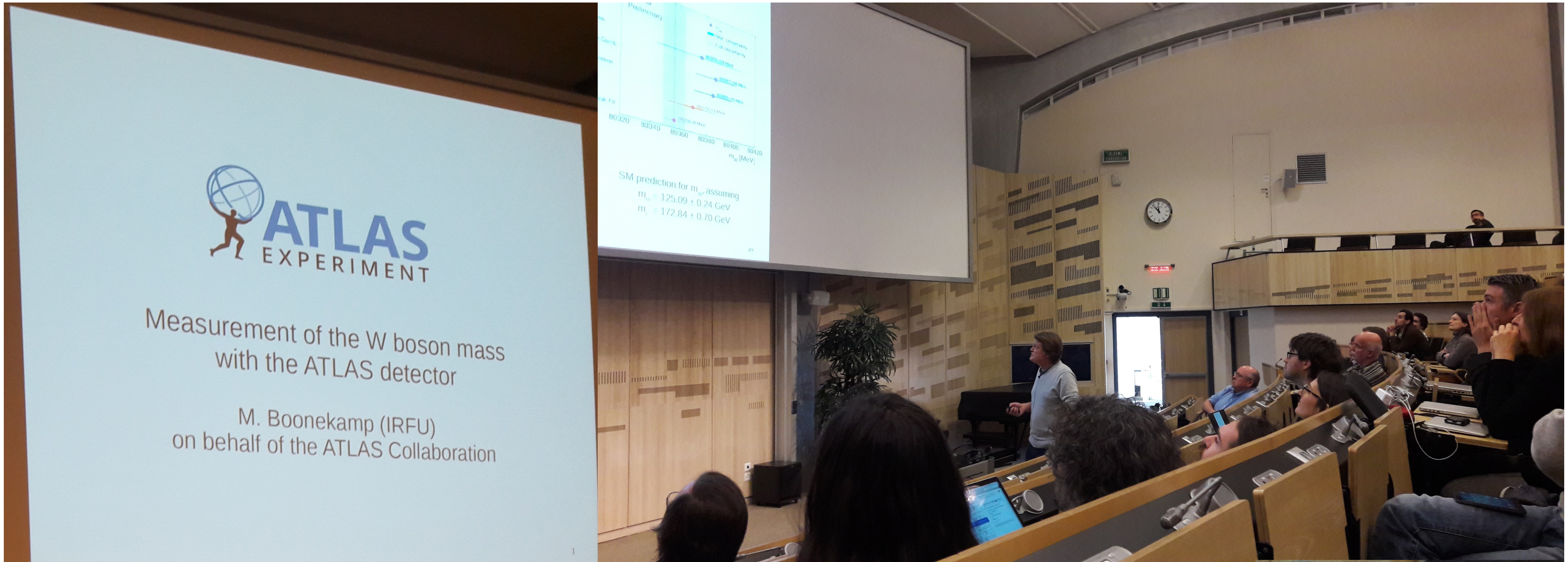

CERN Courier January/February 2017

News

LHC EXPERIMENTS

ATLAS makes precision measurement of W mass

arXiv.org > hep-ex > arXiv:1701.07240v1

arXiv:1701.07240 [hep-ex]

High Energy Physics – Experiment

Measurement of the W–boson mass in pp collisions at $\sqrt{s} = 7$ TeV with the ATLAS detector

ATLAS Collaboration

(Submitted on 25 Jan 2017)

paper is submitted to EPJC

ATLAS detector

Inner detector ($|\eta|< 2.5$, B=2T)
Tracking, vertexing, dE/dx, e/π ID
- Si pixels, Si strips, Trans. Rad. det.
- $\sigma/p_T \sim 3.8\times10^{-4} p_T(\mathrm{GeV}) \oplus 0.015$

Hadron Calorimeter ($|\eta|<5$)
Trigger and meas. of jet/Emiss
- Fe/scintillator (central), Cu/W-LAr (fwd)
- $\sigma/E \sim 50\%/\sqrt{E(\mathrm{GeV})} \oplus 3\%$

4 Magnets Superconducting
- 1 Central solenoid (B=2T)
- 3 Air core Toroids (B=0.5T in the barrel, B=1T in the EC)

EM Calorimeter ($|\eta|<3.2$)
e/γ ID trigger measurement
- Pb-Lar accordion
- $\sigma/E \sim 10\%/\sqrt{E(\mathrm{GeV})} \oplus 1\%$

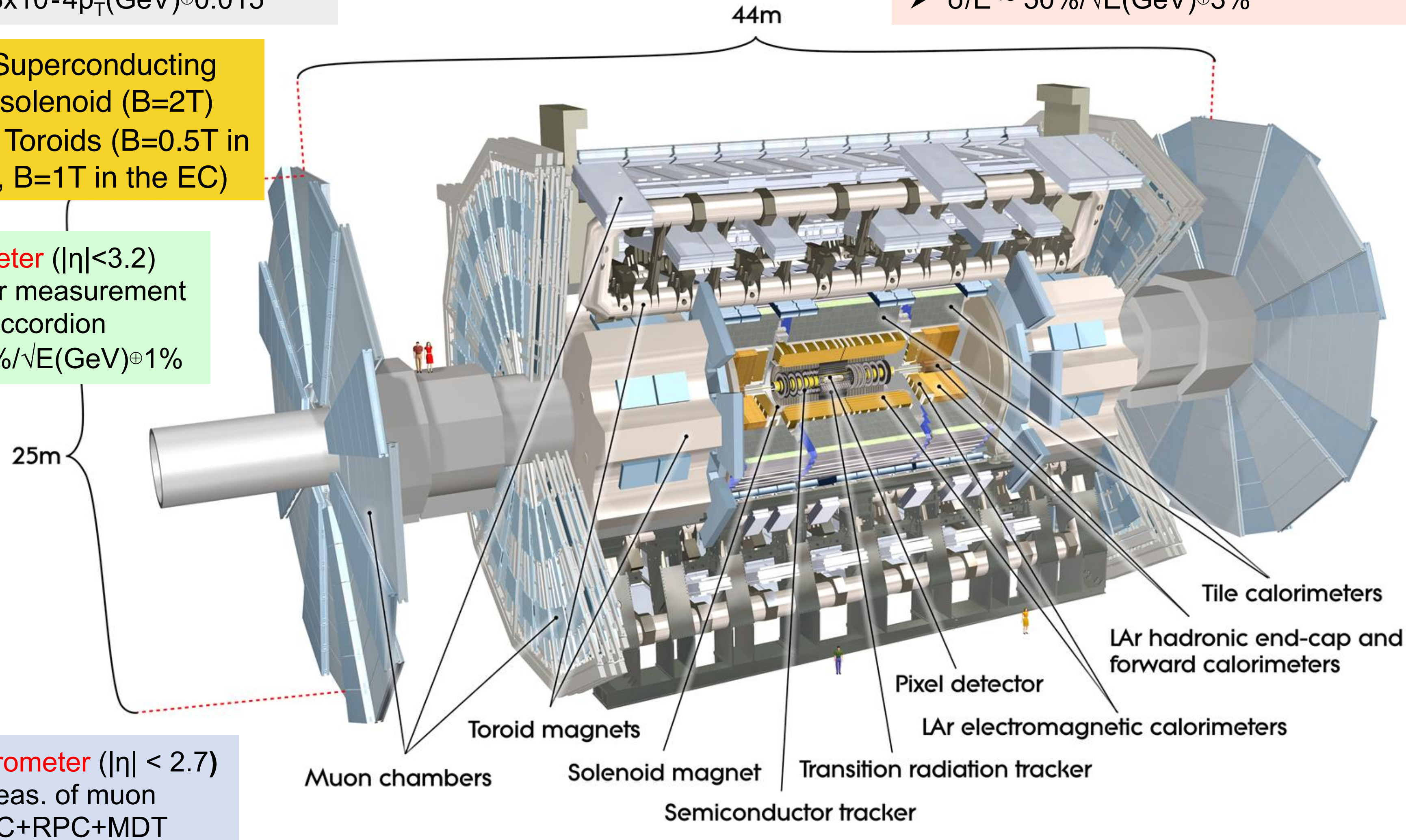

Muon spectrometer ($|\eta| < 2.7$)
Trigger & meas. of muon
- CSC+TGC+RPC+MDT
- σ/p_T <10 % up to 1 TeV

Samples used for the analysis

Data Run I in 2011:

centre-of-mass energy: **7 TeV**
4.6 fb^{-1} for the electron channel
4.1 fb^{-1} for the muon channel
(part of the data discarded due to timing problem in the resistive plate chambers)
bunch spacing: 50 ns

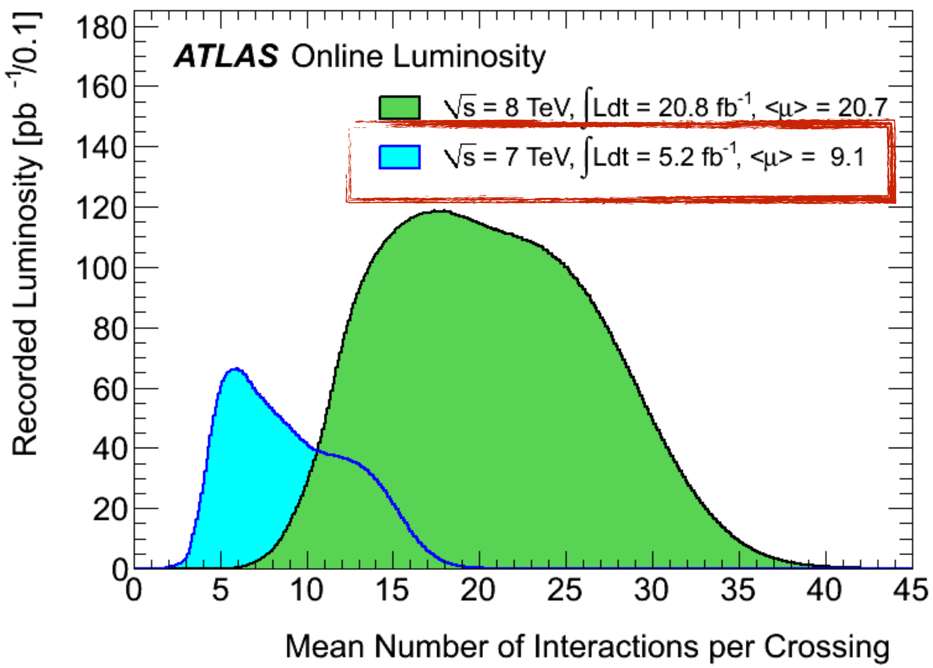

Simulation MC samples:

- Single boson production: **Powheg+Pythia8** (NLO QCD+PS tune AZNLO), QED FSR using PHOTOS
- Herwig and MC@NLO for EW and top backgrounds
- Pile-up simulated using Pythia
- Description of passive material based on final ATLAS Run I calibration results

Selection cuts

Lepton selections:

- muons isolated (track-based) |eta|<2.4
- electrons isolated (track+calorimeter-based) tight identified 0<|eta|<1.2, 1.8<|eta|<2.4

Kinematic requirements: p_T^l>30 GeV, m_T>60 GeV, MET>30 GeV and recoil(u_T)<30 GeV

~6M/8M observed in the electron/muon channel

$\|\eta_\ell\|$ range	0–0.8	0.8–1.4	1.4–2.0	2.0–2.4	Inclusive
$W^+ \to \mu^+\nu$	1 283 332	1 063 131	1 377 773	885 582	4 609 818
$W^- \to \mu^-\bar{\nu}$	1 001 592	769 876	916 163	547 329	3 234 960
$\|\eta_\ell\|$ range	0–0.6	0.6–1.2		1.8–2.4	Inclusive
$W^+ \to e^+\nu$	1 233 960	1 207 136		956 620	3 397 716
$W^- \to e^-\bar{\nu}$	969 170	908 327		610 028	2 487 525

Variables and categories

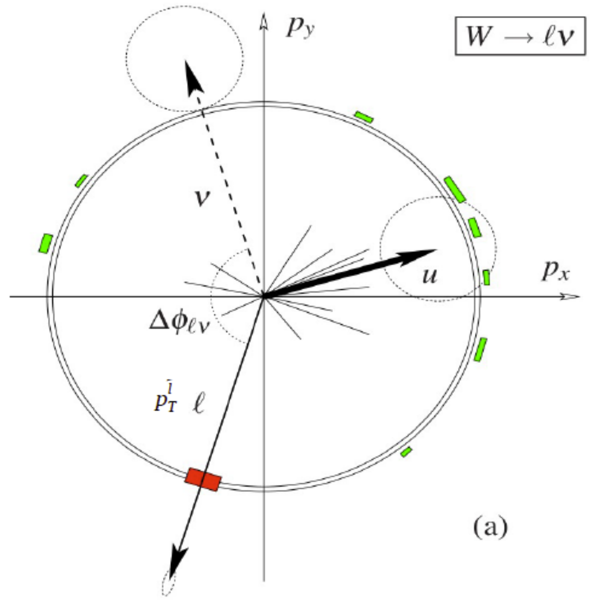

Recoil reconstructed from the vector sum of the momenta of all clusters measured in the calorimeters.

$$\vec{u}_T = \sum_i \vec{E}_{T,i}$$

In W, Z events $-u_T$ provides an estimate of the boson p_T

Sensitive final state distributions: p_T^l, m_T, p_T^{miss} *(not used due to its poor resolution)*

$$\vec{p}_T^{\,miss} = -\left(\vec{p}_T^{\,\ell} + \vec{u}_T\right), \quad m_T = \sqrt{2 p_T^\ell p_T^{miss}(1 - \cos\Delta\phi)}$$

Categories for the measurement:

Decay channel	$W \to e\nu$	$W \to \mu\nu$
Kinematic distributions	p_T^ℓ, m_T	p_T^ℓ, m_T
Charge categories	W^+, W^-	W^+, W^-
$\lvert\eta_\ell\rvert$ categories	$[0, 0.6]$, $[0.6, 1.2]$, $[1.8, 2.4]$	$[0, 0.8]$, $[0.8, 1.4]$, $[1.4, 2.0]$, $[2.0, 2.4]$

Analysis strategy

Template fit approach: compute the p_T^l and m_T distributions for different assumed values of mW —> chi2 minimisation gives the best fit template *(fitting ranges: 32<p_T^l <45 GeV, 66<m_T<99 GeV).*

Predictions for different m_W values are obtained by reweighting the boson invariant mass distribution according to the BW parameterisation.

$$\frac{d\sigma}{dm} \propto \frac{m^2}{(m^2 - m_V^2)^2 + m^4\Gamma_V^2/m_V^2}$$

A blinding offset was applied throughout the measurement and removed when consistent results were found.

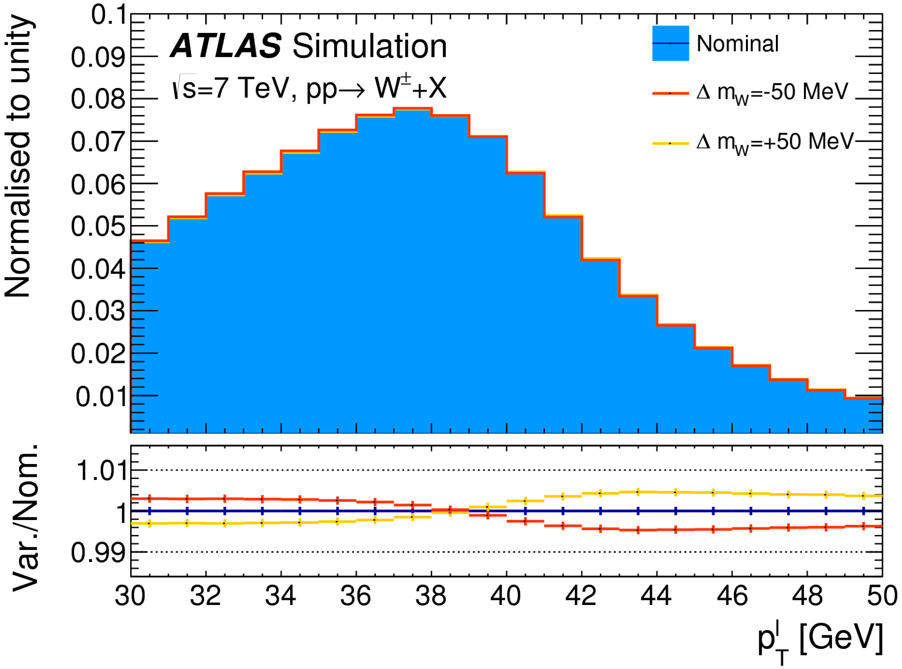

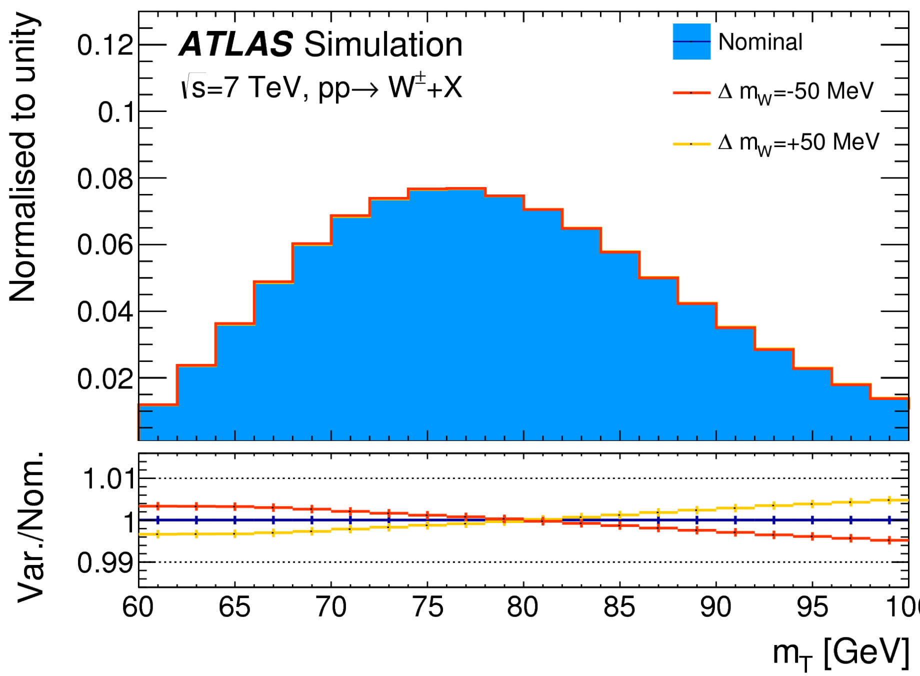

Analysis strategy

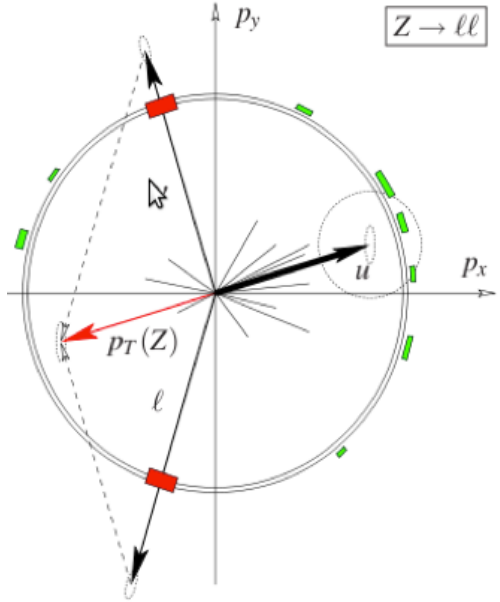

Benefit from the fully reconstructed mass (and kinematics in the transverse plane) in Z-boson sample to validate the analysis and to provide significant experimental and theoretical constraints.

- Lepton momentum corrections derived exploiting the precisely measured value of m_Z at LEP
- The recoil response is calibrated using the expected momentum balance with p_T^{ll} in Z events and tested using the m_T observable
- Ancillary measurements on Z data are used to validate the physics modelling corrections
- The whole analysis is checked by performing a measurement of the Z-boson mass and comparing to the LEP value using:
    - m_{ll} (closure test of the calibration procedure)
    - p_T^l to test the p_T^l-dependence of the corrections and the modelling of the Z p_T and of the relative fractions of the Z-boson helicity states.

Experimental precision

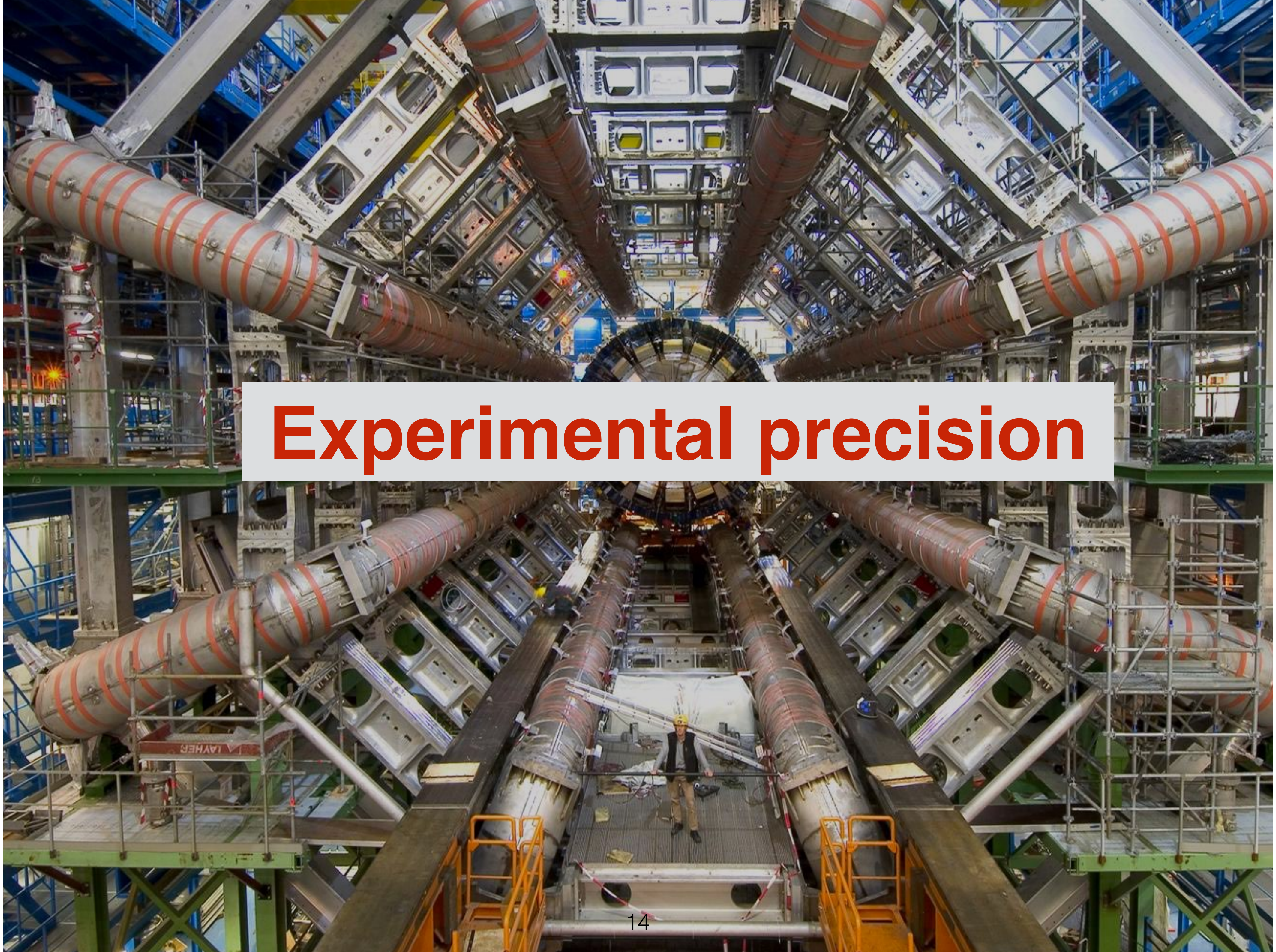

Muon Calibration & Efficiency

Muon identified using combined ID+MS tracks, momentum measurement from ID only.

Calibration factors for ID-only muons derived from Z—>$\mu\mu$ and sagitta bias charge-dependent corrections from Z—>$\mu\mu$ and E/p of W—>eν. [Eur.Phys.J.C 74 (2014) 3130]

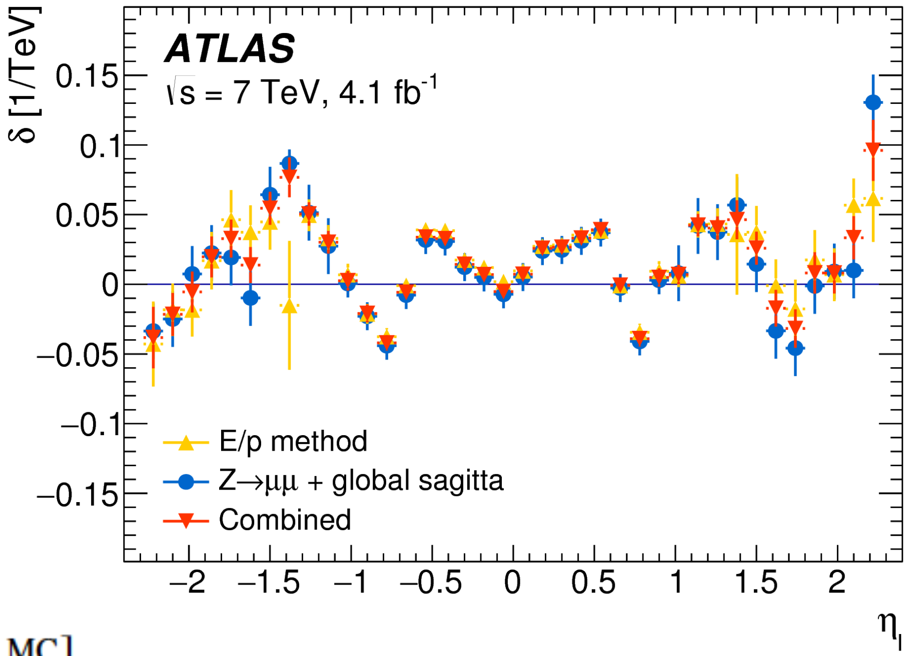

$$p_T^{MC,corr} = p_T^{MC} \times [1+\alpha(\eta,\phi)] \times \left[1+\beta_{curv}(\eta)\cdot G(0,1)\cdot p_T^{MC}\right]$$

$$p_T^{data,corr} = \frac{p_T^{data}}{1+q\cdot\delta(\eta,\phi)\cdot p_T^{data}}$$

Muon trigger/id/iso efficiency corrections data/MC evaluated in bins of p_T^l, eta and charge. Dominant uncertainty is the statistical uncertainty of the Z sample.

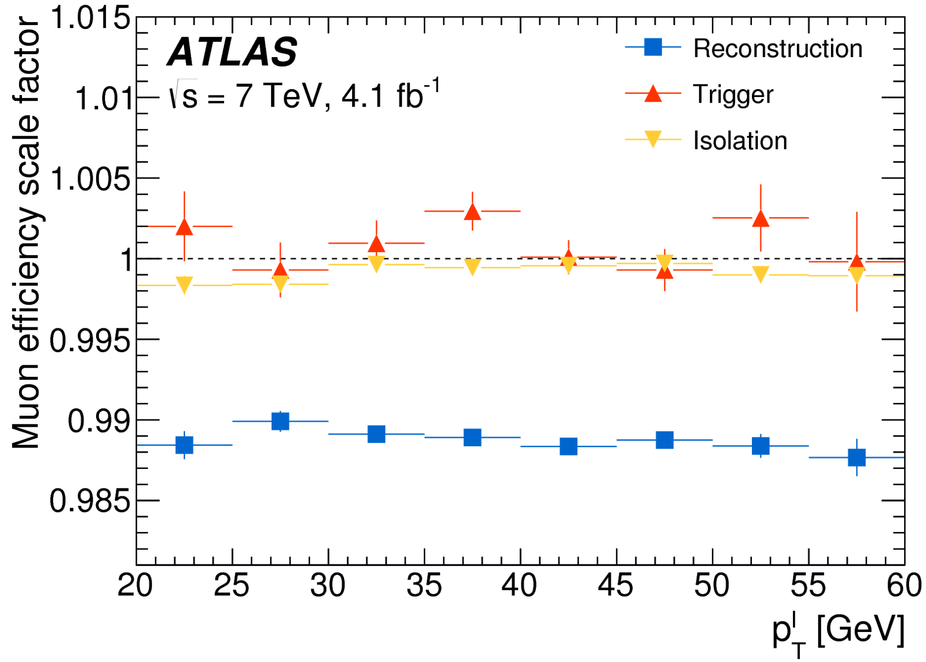

Muon Calibration & Efficiency

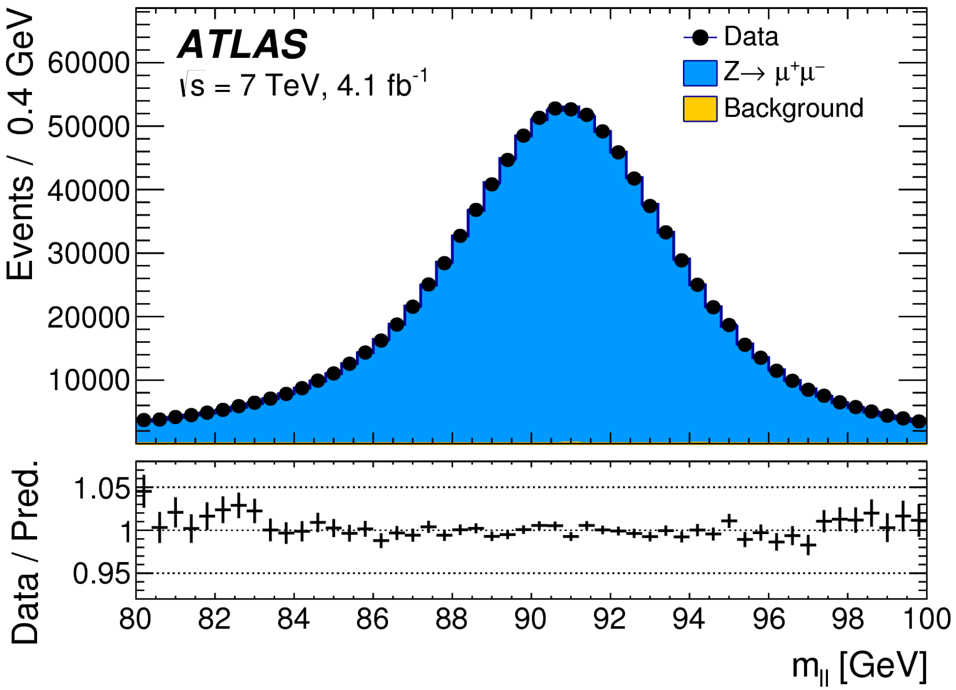

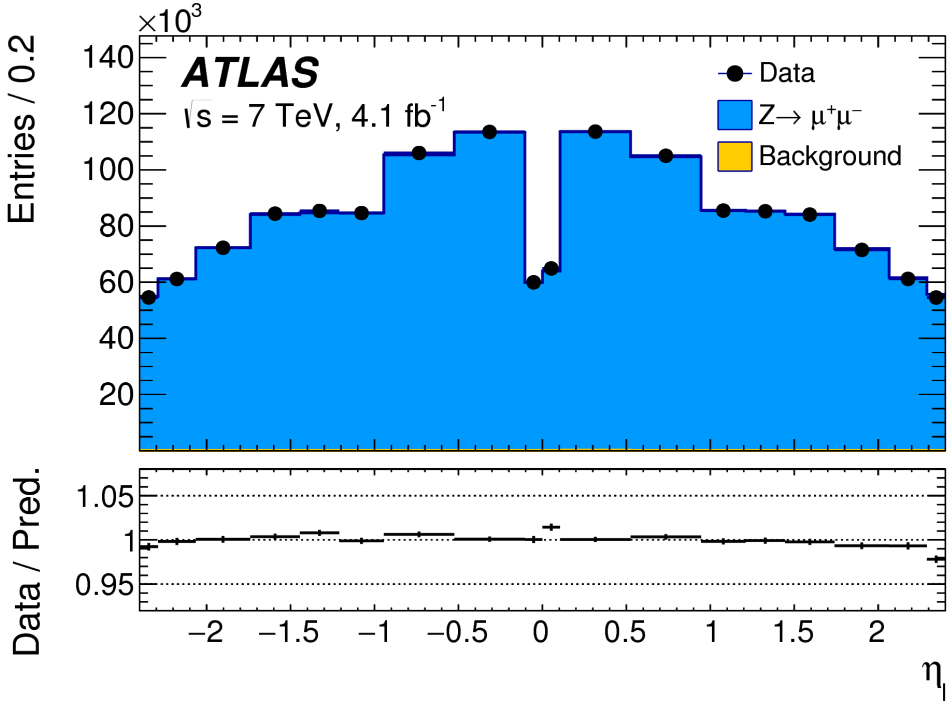

$\vert\eta_\ell\vert$ range	[0.0, 0.8]		[0.8, 1.4]		[1.4, 2.0]		[2.0, 2.4]		Combined	
Kinematic distribution	p_T^ℓ	m_T	p_T^ℓ	m_T	p_T^ℓ	m_T	p_T^ℓ	m_T	p_T^ℓ	m_T
δm_W [MeV]										
Momentum scale	8.9	9.3	14.2	15.6	27.4	29.2	111.0	115.4	8.4	8.8
Momentum resolution	1.8	2.0	1.9	1.7	1.5	2.2	3.4	3.8	1.0	1.2
Sagitta bias	0.7	0.8	1.7	1.7	3.1	3.1	4.5	4.3	0.6	0.6
Reconstruction and isolation efficiencies	4.0	3.6	5.1	3.7	4.7	3.5	6.4	5.5	2.7	2.2
Trigger efficiency	5.6	5.0	7.1	5.0	11.8	9.1	12.1	9.9	4.1	3.2
Total	11.4	11.4	16.9	17.0	30.4	31.0	112.0	116.1	9.8	9.7

Electron Calibration & Efficiency

Calibration for electrons closely follows the Run I calibration paper [Eur.Phys.J.C 74 (2014) 3071]

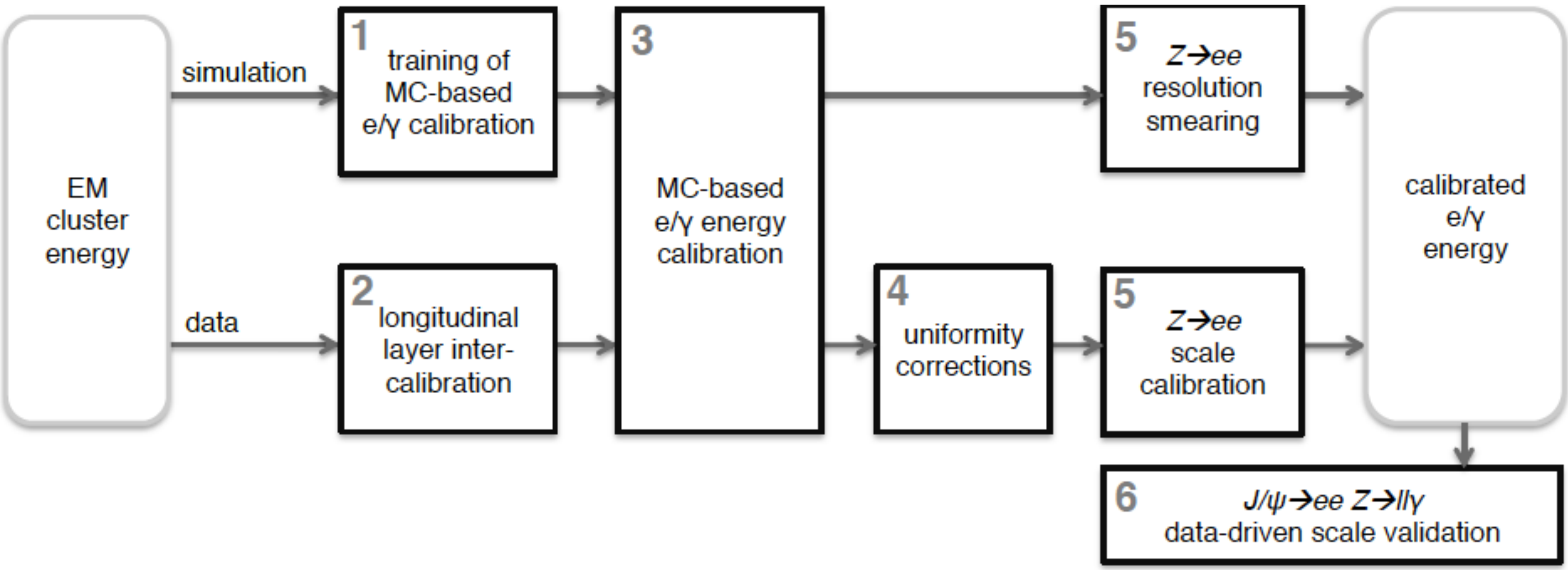

Exclude bin 1.2<|eta|<1.82 for the W mass measurement as the amount of passive material in front of the calorimeter and its uncertainty are largest in this region.
Azimuthal correction from <E/p> vs phi

Electron efficiency corrections en fonction de eta et p_T [Eur.Phys.J.C 74 (2014) 2941]

Electron Calibration & Efficiency

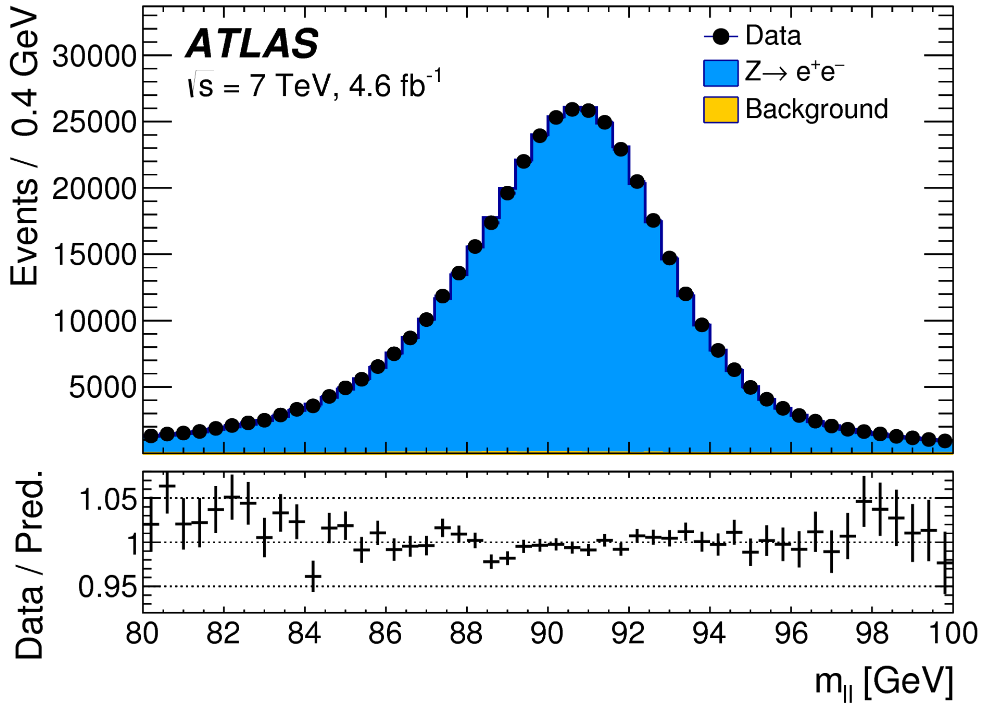

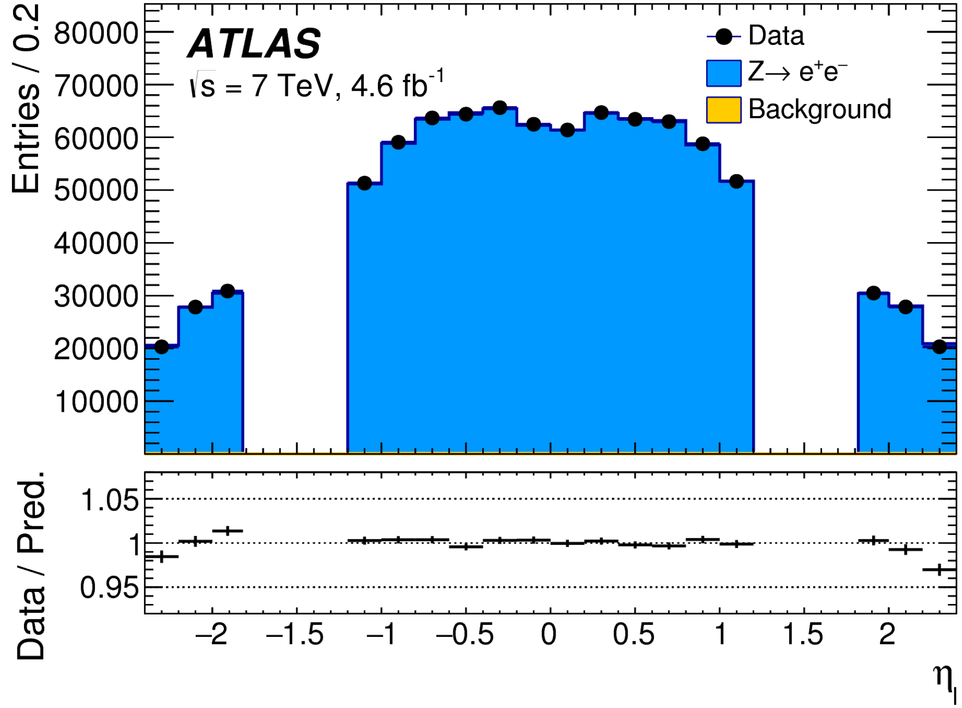

$\|\eta_\ell\|$ range	[0.0, 0.6]		[0.6, 1.2]		[1.82, 2.4]		Combined	
Kinematic distribution	p_T^ℓ	m_T	p_T^ℓ	m_T	p_T^ℓ	m_T	p_T^ℓ	m_T
δm_W [MeV]								
Energy scale	10.4	10.3	10.8	10.1	16.1	17.1	8.1	8.0
Energy resolution	5.0	6.0	7.3	6.7	10.4	15.5	3.5	5.5
Energy linearity	2.2	4.2	5.8	8.9	8.6	10.6	3.4	5.5
Energy tails	2.3	3.3	2.3	3.3	2.3	3.3	2.3	3.3
Reconstruction efficiency	10.5	8.8	9.9	7.8	14.5	11.0	7.2	6.0
Identification efficiency	10.4	7.7	11.7	8.8	16.7	12.1	7.3	5.6
Trigger and isolation efficiencies	0.2	0.5	0.3	0.5	2.0	2.2	0.8	0.9
Charge mismeasurement	0.2	0.2	0.2	0.2	1.5	1.5	0.1	0.1
Total	19.0	17.5	21.1	19.4	30.7	30.5	14.2	14.3

Recoil Calibration

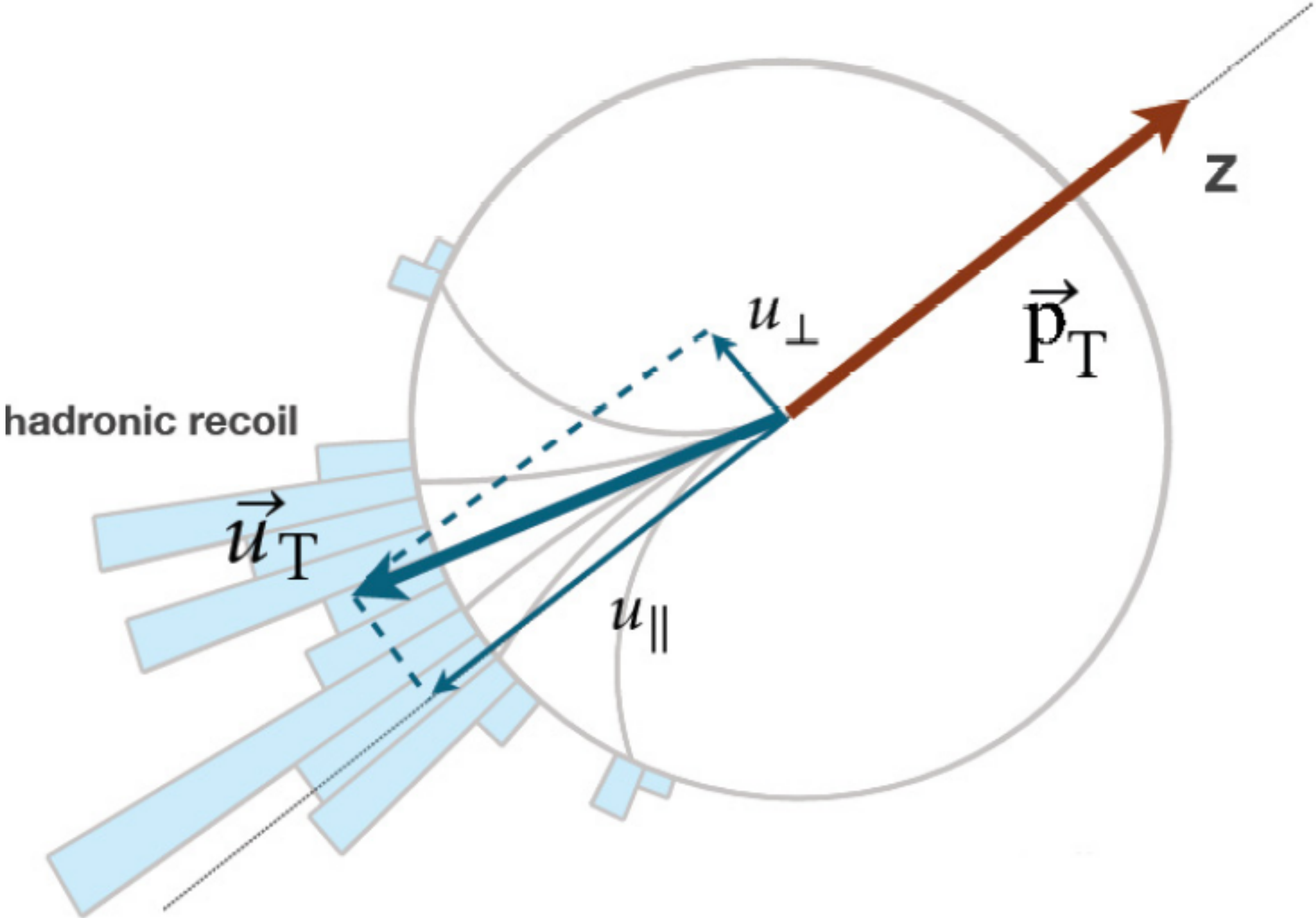

Recoil Calibration

A set of corrections is derived:

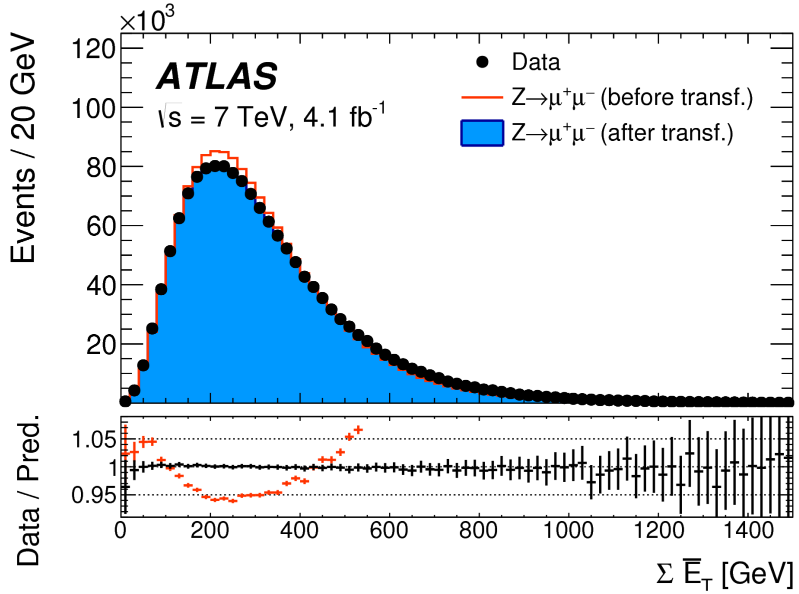

- equalise pile-up multiplicity distribution in data and MC
- equalise SumE$_T$-u for W$^+$,W$^-$,Z in data and MC
- apply residual recoil energy scale and resolution corrections using p$_T$ balance in Z events (in bins of p$_T^{ll}$ and SumE$_T$-u)

The corrections are derived in pile-up bins, <*μ*>, 2.5-6.5, 6.5-9.5 and 9.5-16.0

A closure test of the applicability of Z-based corrections to W production is performed using Powheg+Herwig6 samples.

The particle-level p$_T$(W) distribution in Powheg+Pythia8 is reweighted to Powheg+Herwig6

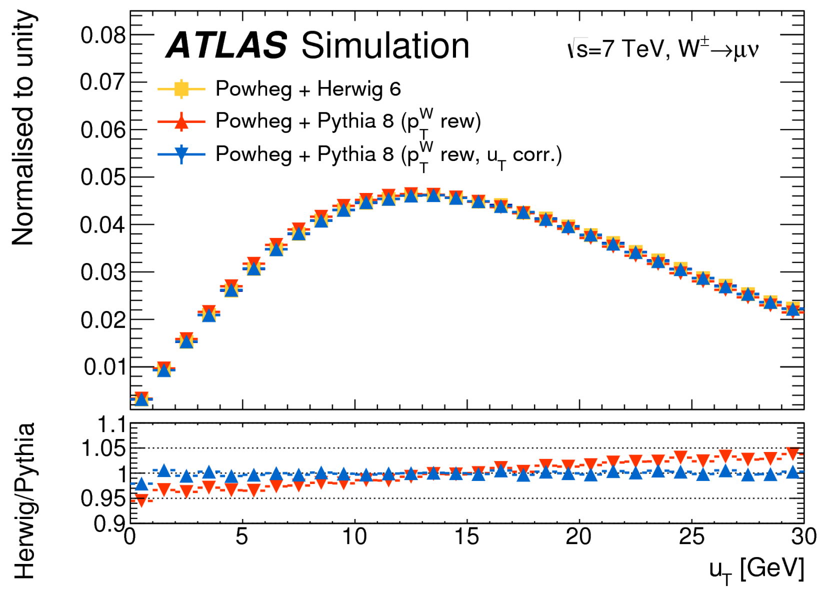

Recoil Calibration

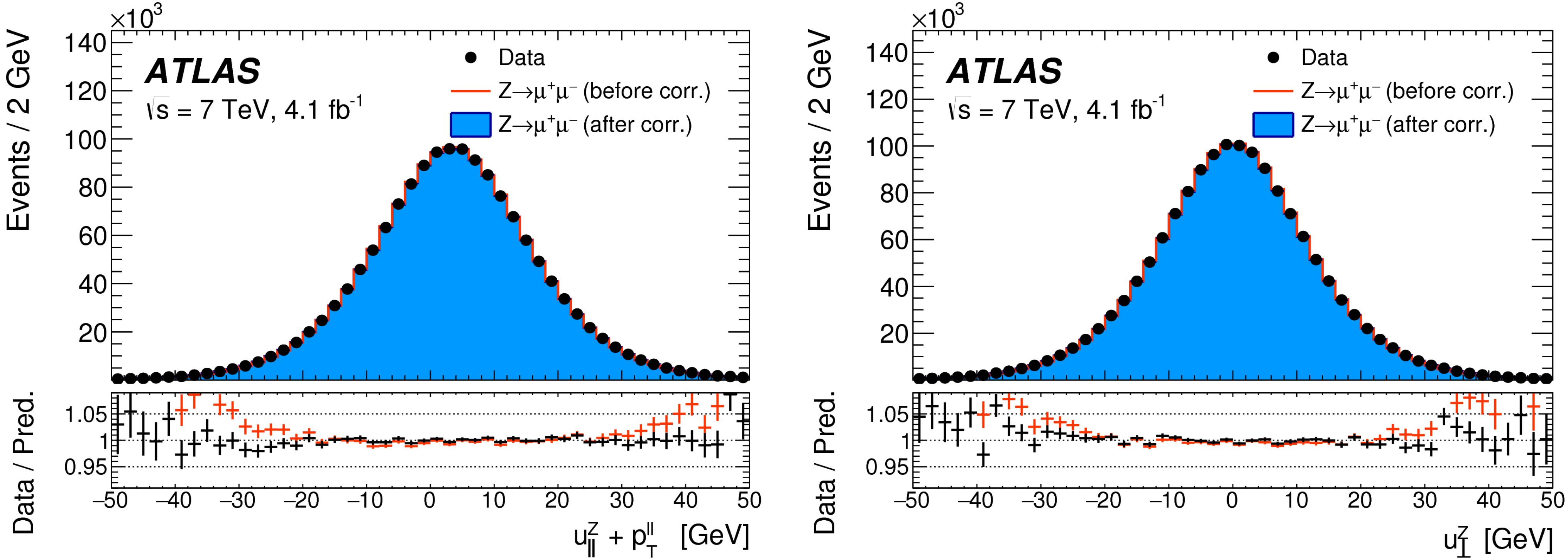

W-boson charge	W^+		W^-		Combined	
Kinematic distribution	p_T^ℓ	m_T	p_T^ℓ	m_T	p_T^ℓ	m_T
δm_W [MeV]						
$\langle\mu\rangle$ scale factor	0.2	1.0	0.2	1.0	0.2	1.0
$\Sigma\bar{E}_T$ correction	0.9	12.2	1.1	10.2	1.0	11.2
Residual corrections (statistics)	2.0	2.7	2.0	2.7	2.0	2.7
Residual corrections (interpolation)	1.4	3.1	1.4	3.1	1.4	3.1
Residual corrections ($Z \to W$ extrapolation)	0.2	5.8	0.2	4.3	0.2	5.1
Total	2.6	14.2	2.7	11.8	2.6	13.0

Physics modelling

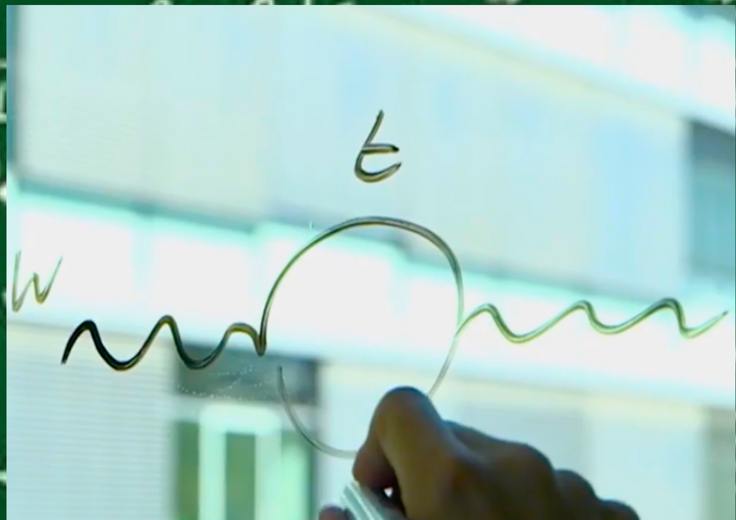

Physics modelling

No available single generator to describe all the physics modelling

Start from the Powheg+Pythia8 and apply corrections. Use ancillary measurements of Drell-Yan processes to validate (and tune) the model and assess systematic uncertainties.

Physics modelling corrections

Electroweak corrections

- *QED FSR and ISR*
- *missing higher order effects*
- *FSR pair production*

QCD corrections

- *pT distribution*
- *polarisation*
- *rapidity*

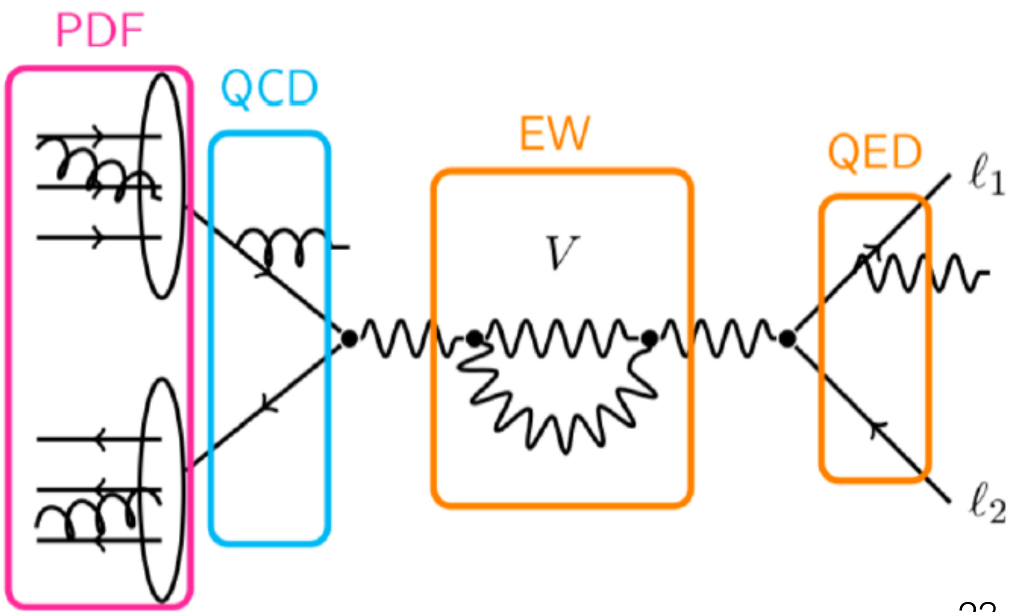

EW corrections

QED effects: FSR *(dominant correction)* included in the simulation with PHOTOS, negligible uncertainty. QED ISR included through Pythia8 parton shower.

NLO EW effects: taken as uncertainties, pure weak corrections evaluated in the presence of QCD corrections, estimated using Winhac. ISR-FSR interference.

FSR lepton pair production estimated and added as an uncertainty. Formally higher order correction but a significant additional source of energy loss.

Decay channel	$W \to e\nu$		$W \to \mu\nu$	
Kinematic distribution	p_T^ℓ	m_T	p_T^ℓ	m_T
δm_W [MeV]				
FSR (real)	< 0.1	< 0.1	< 0.1	< 0.1
Pure weak and IFI corrections	3.3	2.5	3.5	2.5
FSR (pair production)	3.6	0.8	4.4	0.8
Total	4.9	2.6	5.6	2.6

QCD corrections

The Drell-Yan cross-section can be decomposed by factorising the dynamic of the boson production and the kinematic of the boson decay. An approximate decomposition is given by:

$$\frac{d\sigma}{dp_1\,dp_2} = \left[\frac{d\sigma(m)}{dm}\right]\left[\frac{d\sigma(y)}{dy}\right]\left[\frac{d\sigma(p_T, y)}{dp_T\,dy}\left(\frac{d\sigma(y)}{dy}\right)^{-1}\right]\left[(1+\cos^2\theta) + \sum_{i=0}^{7} A_i(p_T, y) P_i(\cos\theta, \phi)\right]$$

Breit-Wigner

NNLO pQCD

Parton Shower

The dσ/dm is modelled with a BW parametrisation (+ EW corrections)
The dσ/dy and the Ai coefficients are modelled with fixed order pQCD at NNLO
The dσ/dp_T is modelled with parton shower (tried analytic resummation)

Rapidity distribution

The rapidity distribution is modelled with NNLO predictions and the CT10nnlo PDF set. PDF choice validated on the observed weaker suppression of the strange quark in the W,Z cross-section data as published in arXiv:1612.03016

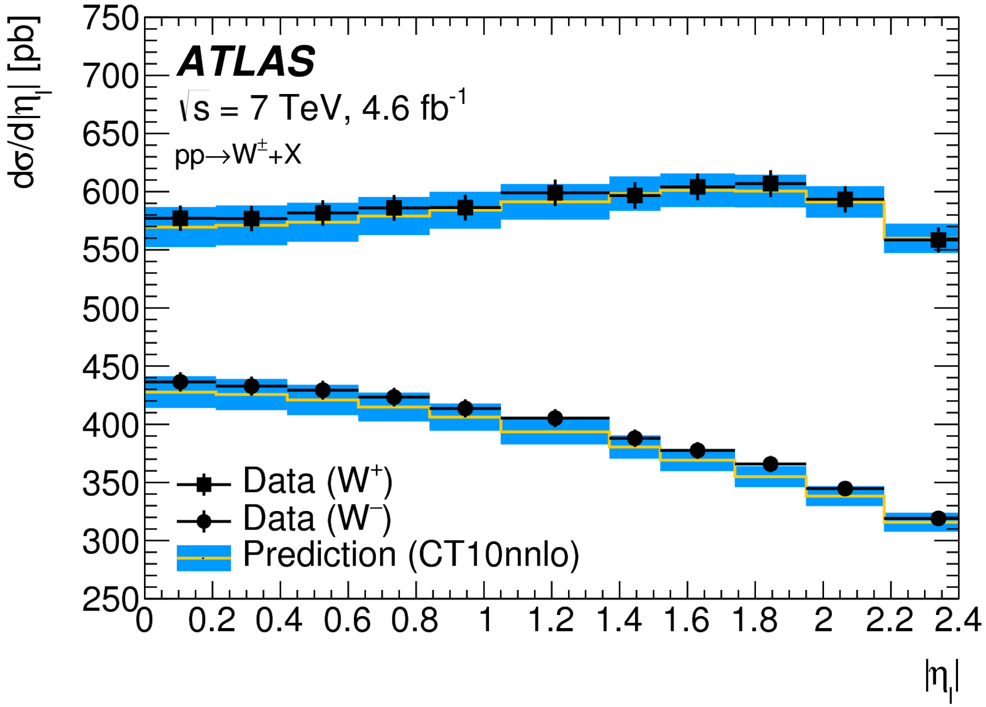

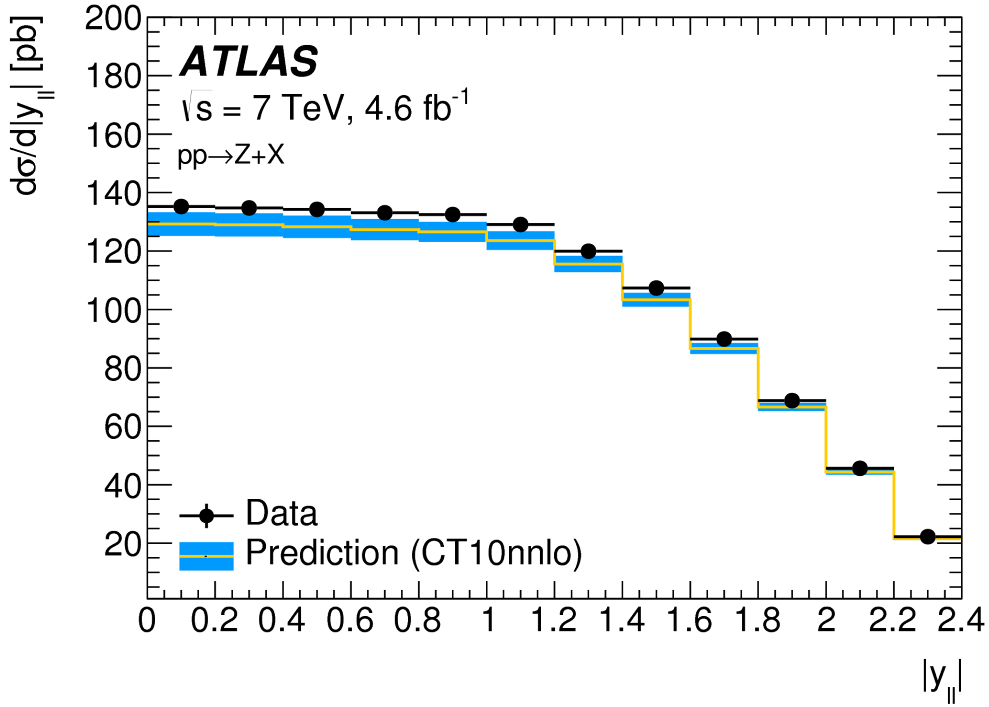

Satisfactory agreement between the theoretical prediction and the measurements is observed: $\chi^2/\mathrm{dof} = 45/34$.

Angular coefficients

The Ai coefficients are modelled with fixed order pQCD at NNLO.
The predictions (DYNNLO) are validated by comparison to the Ai measurements in 8 TeV Z-boson data JHEP08(2016)159

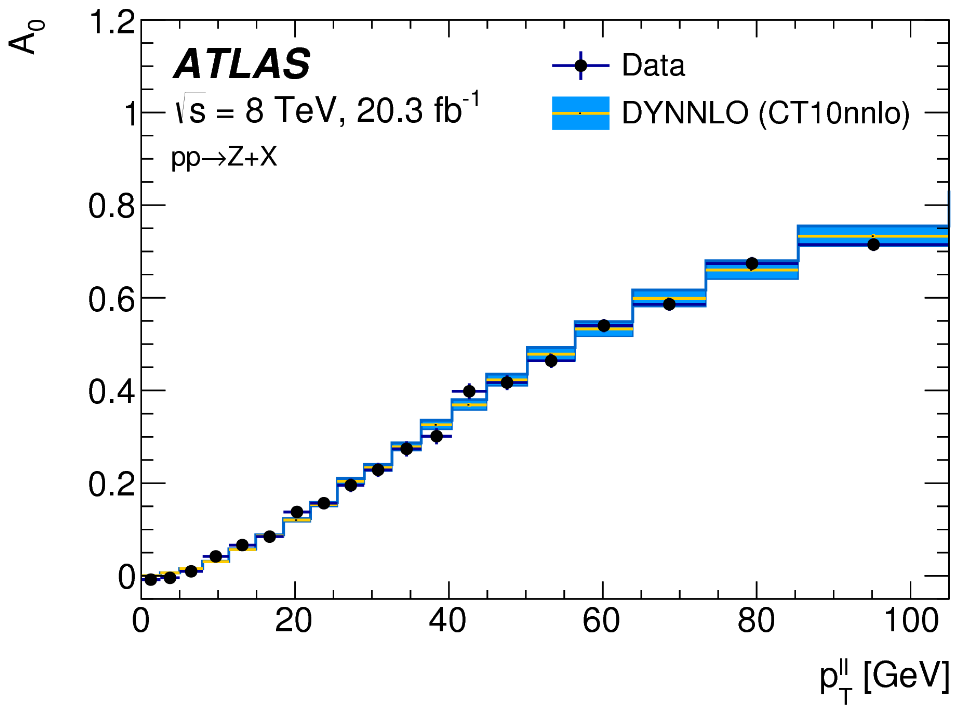

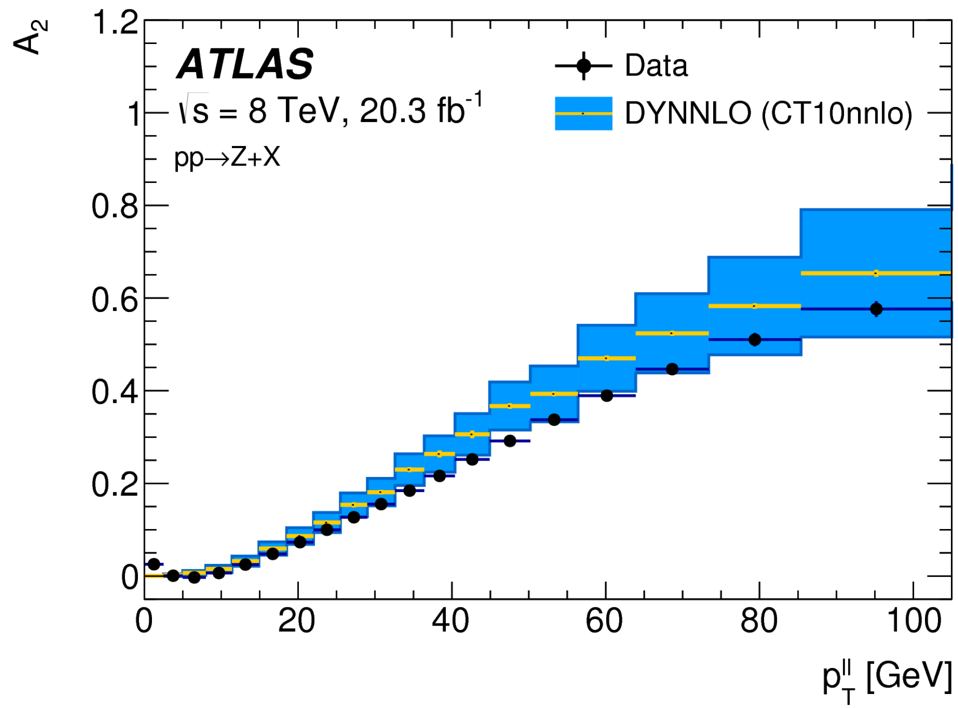

Uncertainties on Ai modelling: experimental uncertainty of the measurement and observed discrepancy for A2 coefficient

W-boson charge	W^+		W^-		Combined	
Kinematic distribution	p_T^ℓ	m_T	p_T^ℓ	m_T	p_T^ℓ	m_T
Angular coefficients	5.8	5.3	5.8	5.3	5.8	5.3

Transverse momentum

Parton shower MC Pythia 8 tuned to the 7 TeV data AZ tune (better description in rapidity bins then the AZNLO tune of Powheg+Pythia) JHEP09(2014)145

	PYTHIA8
Tune Name	AZ
Primordial k_T [GeV]	1.71 ± 0.03
ISR $\alpha_S^{ISR}(m_Z)$	0.1237 ± 0.0002
ISR cut-off [GeV]	0.59 ± 0.08
χ^2_{min}/dof	45.4/32

The agreement between data and Pythia AZ is better than 1% for p_T<40 GeV

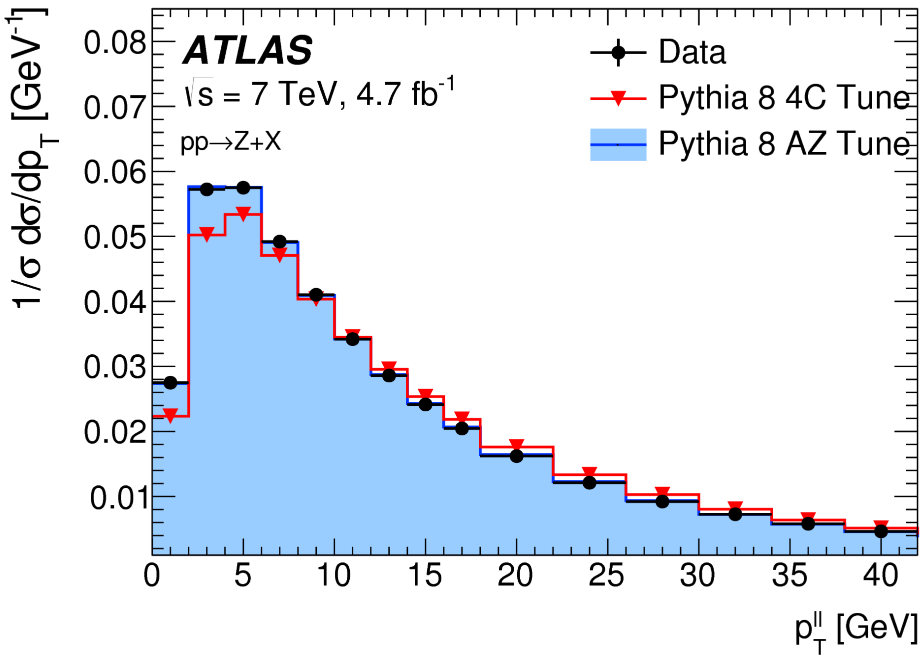

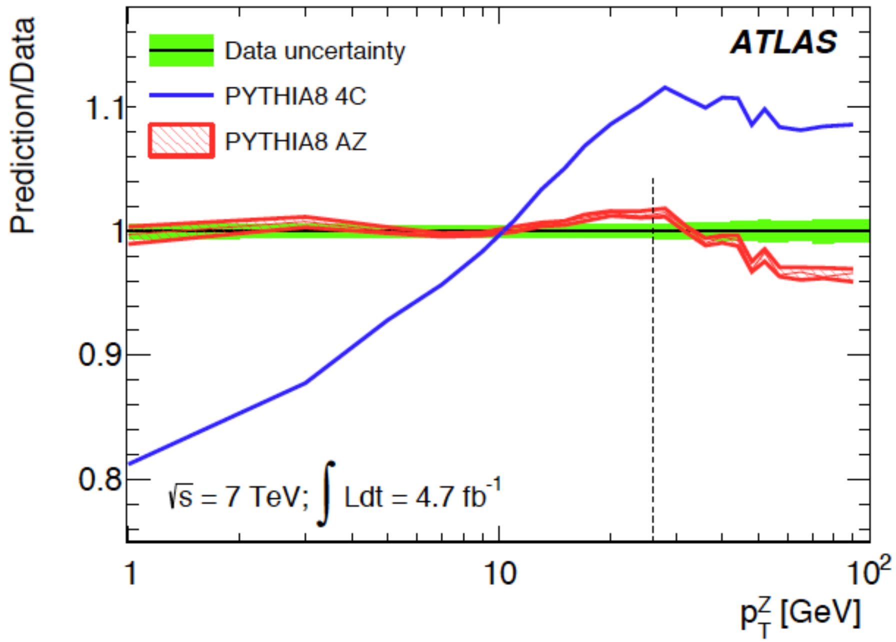

The accuracy of Z data is propagated and considered as an uncertainty

W-boson charge	W^+		W^-		Combined	
Kinematic distribution	p_T^ℓ	m_T	p_T^ℓ	m_T	p_T^ℓ	m_T
AZ tune	3.0	3.4	3.0	3.4	3.0	3.4

Transverse momentum

Resummed predictions (DYRES, ResBos, CuTe) and Powheg MiNLO+Pythia8 were tried but they predict harder W p_T spectrum for a given p_T (Z) spectrum.

truth-level

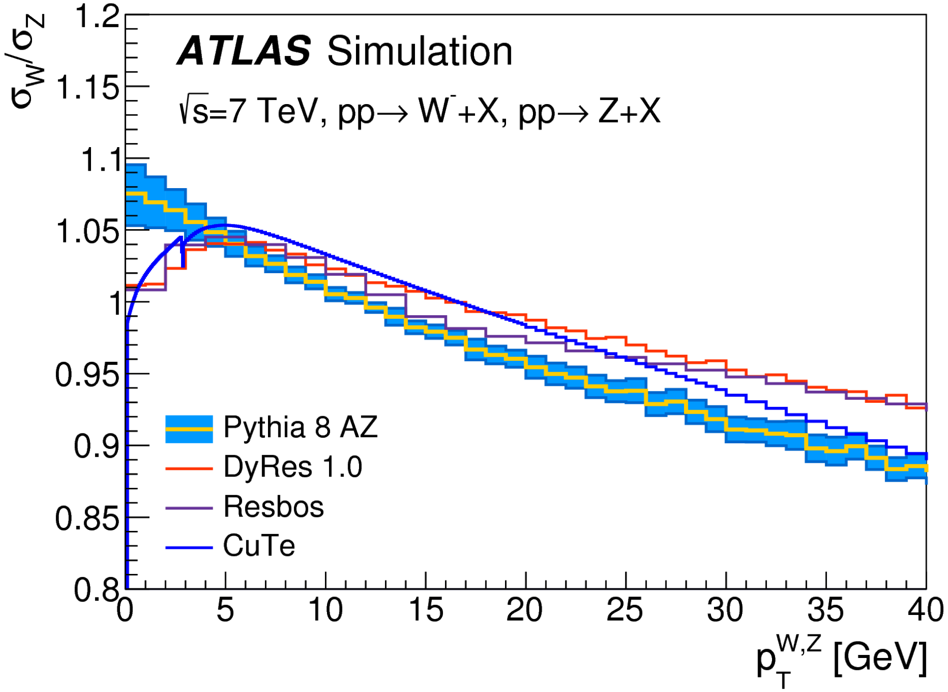

reco-level

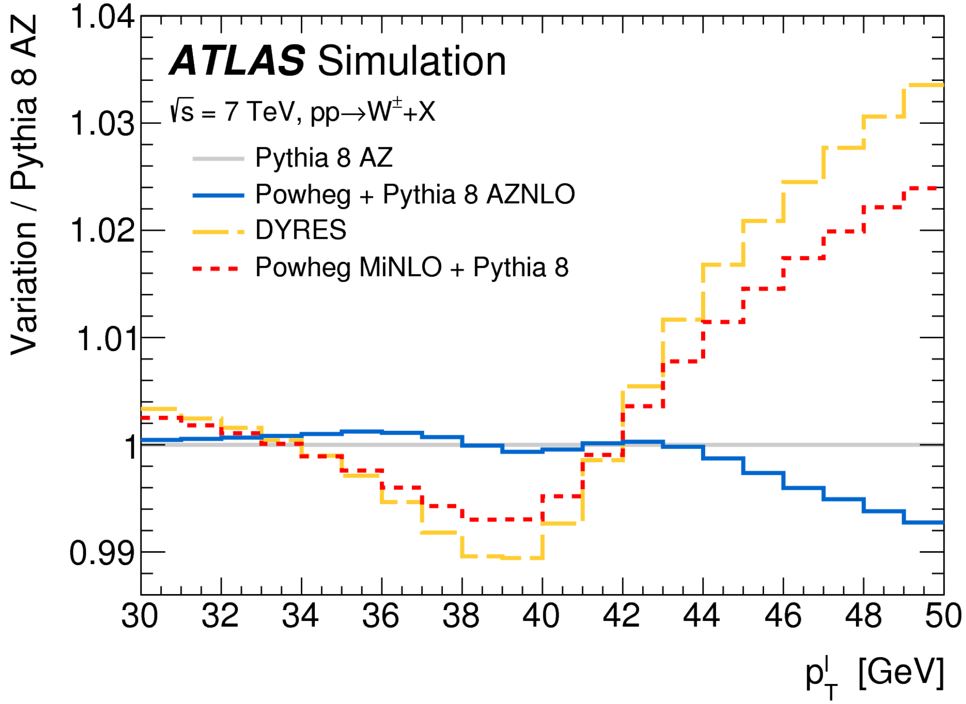

The effect on m_W of using the "formally" more accurate predictions has a significant impact on the W-mass value of the order of 50-100 MeV

Transverse momentum

The $u_{||}(l)$ distribution is very sensitive to the underlying $p_T(W)$ distribution

—> used to provide a data-driven validation of the accuracy of our Pythia8 AZ model and to compare to the other calculations

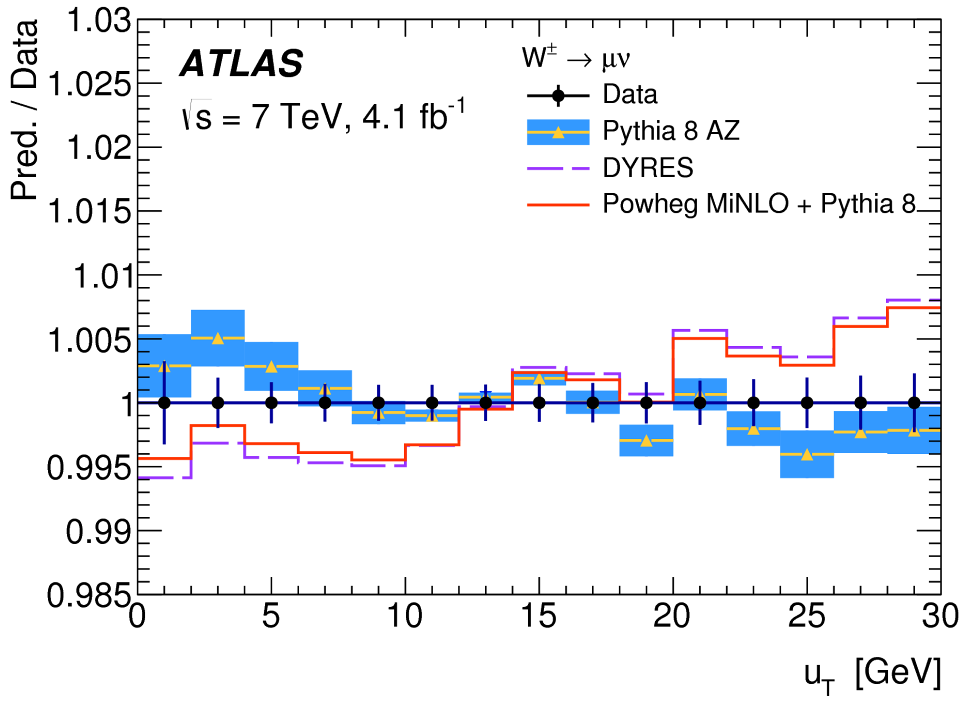

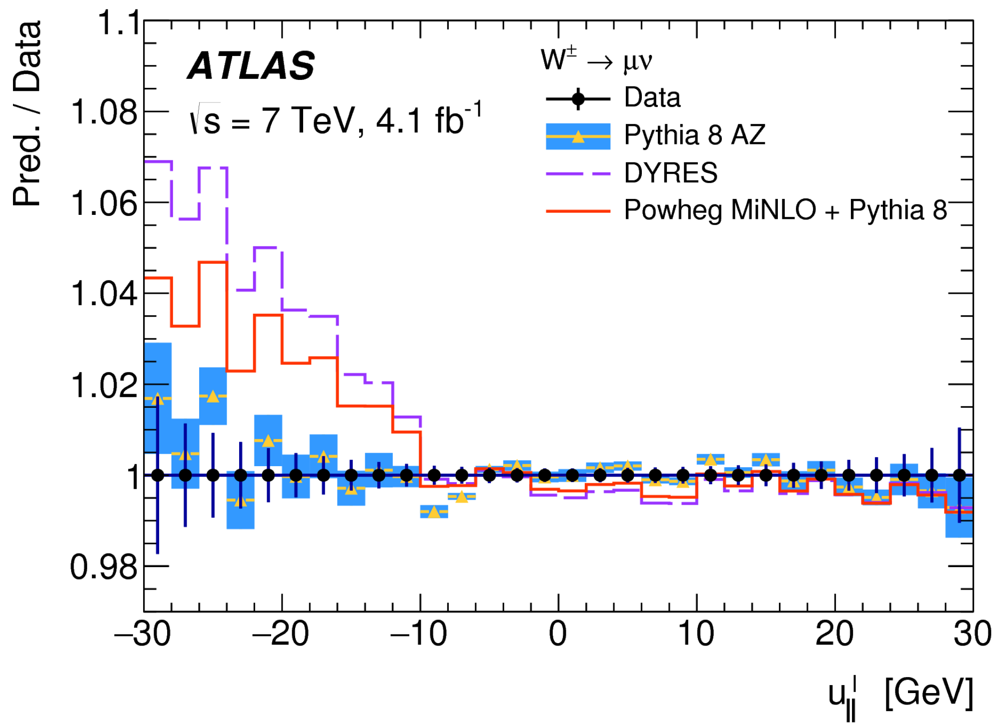

The NNLL resummed predictions and Powheg+MiNLO are strongly disfavoured by the data and the PS MC are in a good agreement tested using Pythia8 , Herwig7 and Powheg+Pythia8

Transverse momentum uncertainties

Z—>W extrapolation: heavy quark masses *(varying m_c by ±0.5 GeV and m_b by ±0.8 GeV)*, factorisation scale variations in the QCD ISR *(separately for light and heavy-quark induced production)*,

Relative variations of the $p_T(W)$ and $p_T(Z)$ are considered.

Higher-order QCD expected to be largely correlated between W and Z produced by light quarks but a certain degree of decorrelation is expected from heavy-flavour induced production.

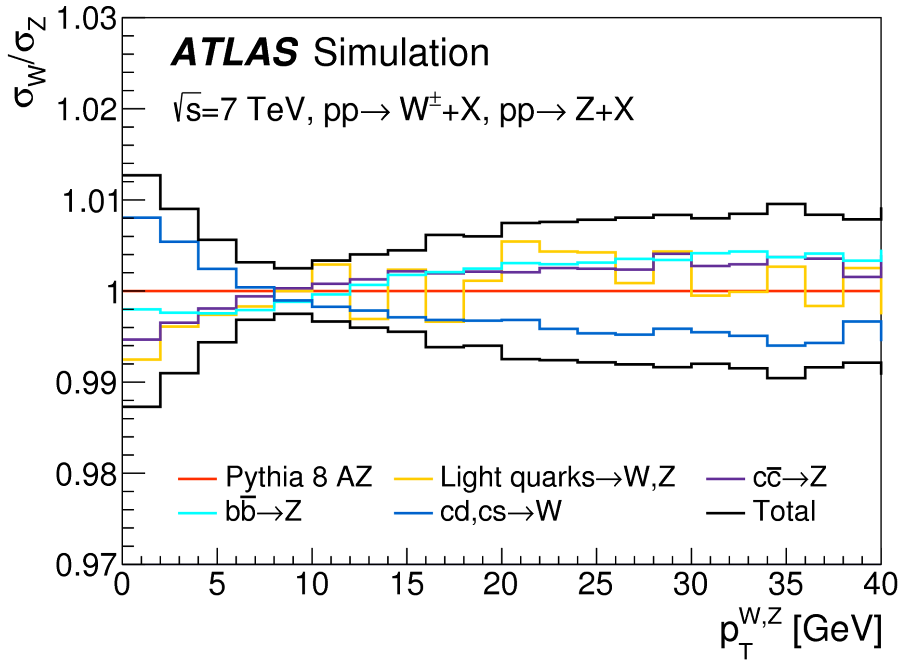

W-boson charge	W^+		W^-		Combined	
Kinematic distribution	p_T^ℓ	m_T	p_T^ℓ	m_T	p_T^ℓ	m_T
Charm-quark mass	1.2	1.5	1.2	1.5	1.2	1.5
Parton shower μ_F with heavy-flavour decorrelation	5.0	6.9	5.0	6.9	5.0	6.9

PDF uncertainties

PDF variations (25 error eigenvectors) of CT10nnlo are applied simultaneously to the boson rapidity, Ai, and p_T distributions.

Only relative variations of the $p_T(W)$ and $p_T(Z)$ induced by PDFs are considered.

Consider largest deviation of $p_T(W)/p_T(Z)$ for the parton shower PDF variation: CTEQ6L1 LO (nominal) to CT14lo, MMHT2014lo and NNPDF2.3lo

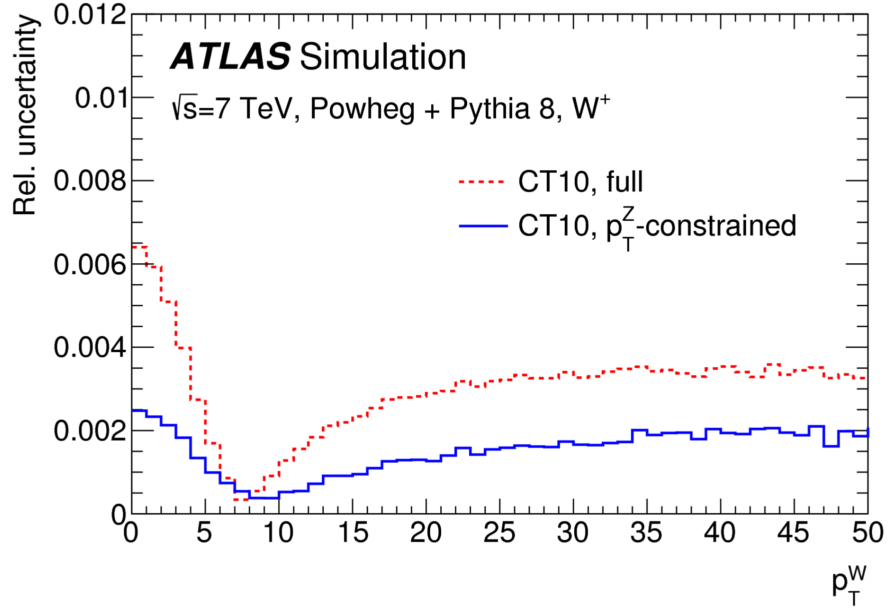

W-boson charge	W^+		W^-		Combined	
Kinematic distribution	p_T^ℓ	m_T	p_T^ℓ	m_T	p_T^ℓ	m_T
Fixed-order PDF uncertainty	13.1	14.9	12.0	14.2	8.0	8.7
Parton shower PDF uncertainty	3.6	4.0	2.6	2.4	1.0	1.6

The PDF uncertainties very similar between p_T^l and m_T but strongly anti-correlated between W^+ and W^-. Envelope taken from CT14 and MMHT2014~3.8 MeV.

Summary of physics modelling uncertainties

W-boson charge	W^+		W^-		Combined	
Kinematic distribution	p_T^ℓ	m_T	p_T^ℓ	m_T	p_T^ℓ	m_T
δm_W [MeV]						
Fixed-order PDF uncertainty	13.1	14.9	12.0	14.2	8.0	8.7
AZ tune	3.0	3.4	3.0	3.4	3.0	3.4
Charm-quark mass	1.2	1.5	1.2	1.5	1.2	1.5
Parton shower μ_F with heavy-flavour decorrelation	5.0	6.9	5.0	6.9	5.0	6.9
Parton shower PDF uncertainty	3.6	4.0	2.6	2.4	1.0	1.6
Angular coefficients	5.8	5.3	5.8	5.3	5.8	5.3
Total	15.9	18.1	14.8	17.2	11.6	12.9

QCD

Decay channel	$W \to e\nu$		$W \to \mu\nu$	
Kinematic distribution	p_T^ℓ	m_T	p_T^ℓ	m_T
δm_W [MeV]				
FSR (real)	< 0.1	< 0.1	< 0.1	< 0.1
Pure weak and IFI corrections	3.3	2.5	3.5	2.5
FSR (pair production)	3.6	0.8	4.4	0.8
Total	4.9	2.6	5.6	2.6

EW

The PDF uncertainties are the dominant followed by $p_T(W)$ uncertainty due to the heavy-flavour initiated production.

Validation and results

Cross checks with Z events

Z tranverse momentum and rapidity distributions in e, mu channels

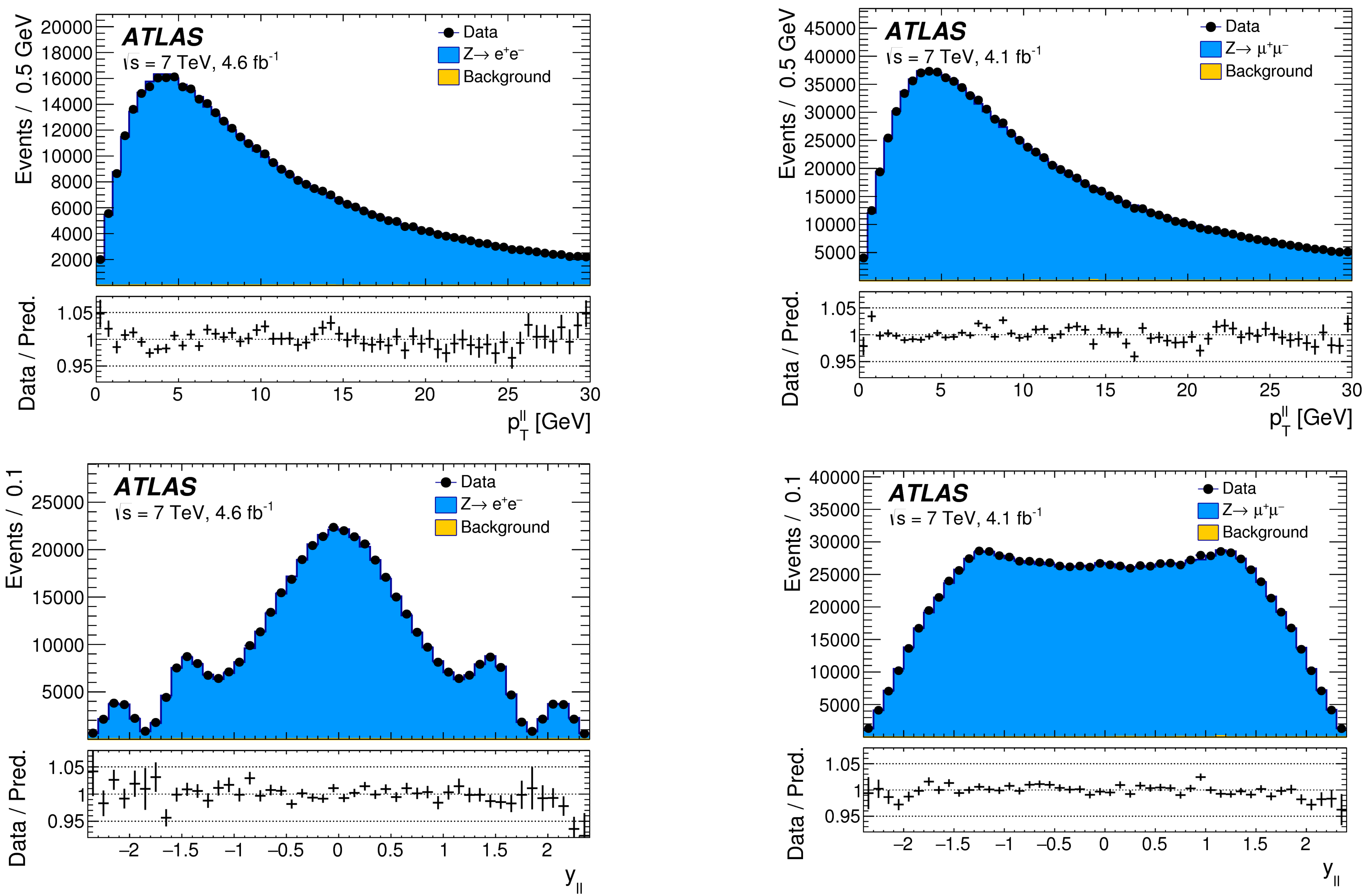

Good agreement is observed. Error bars are statistics only.

Cross checks with Z events

Tranverse momentum and transverse mass distributions in e, mu channels

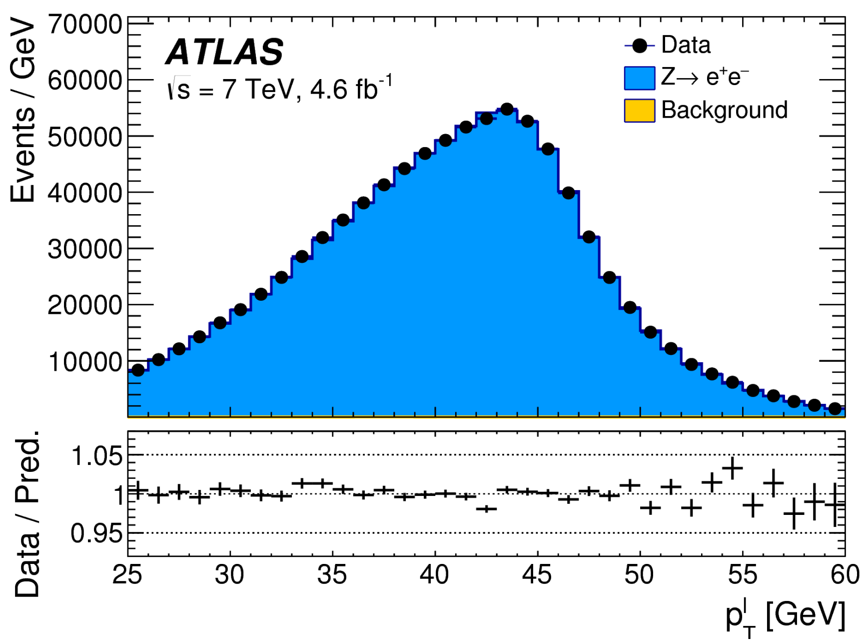

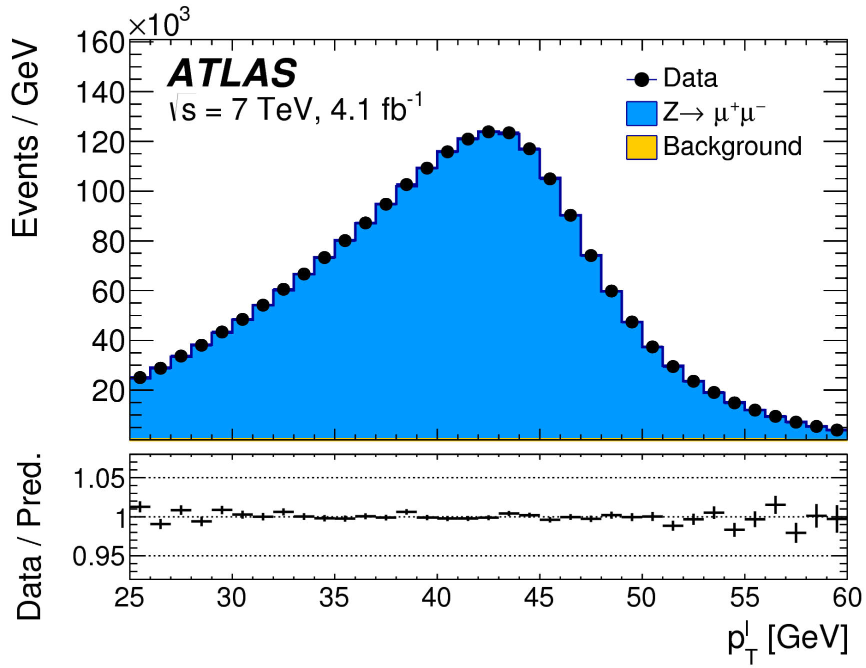

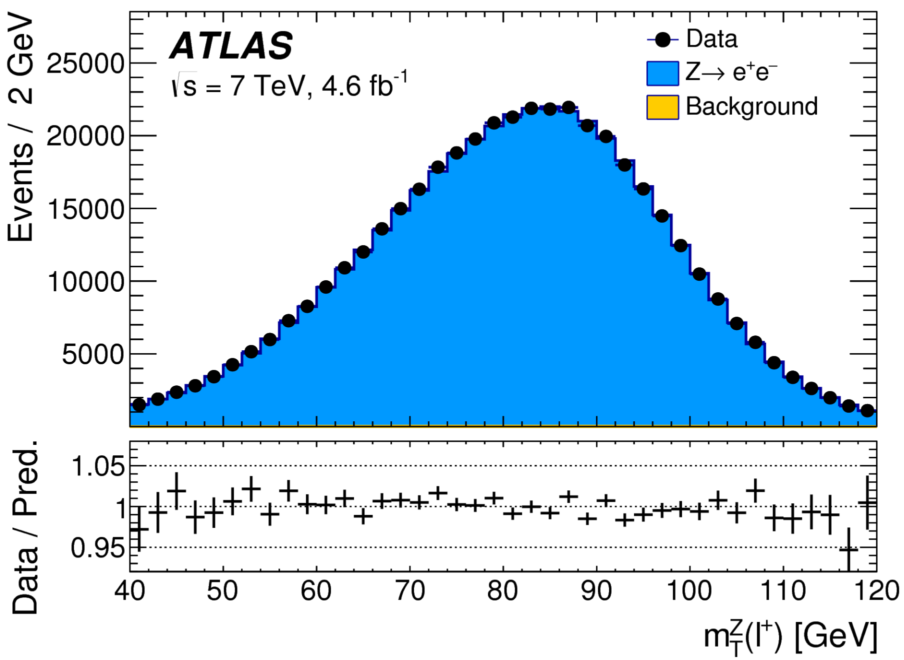

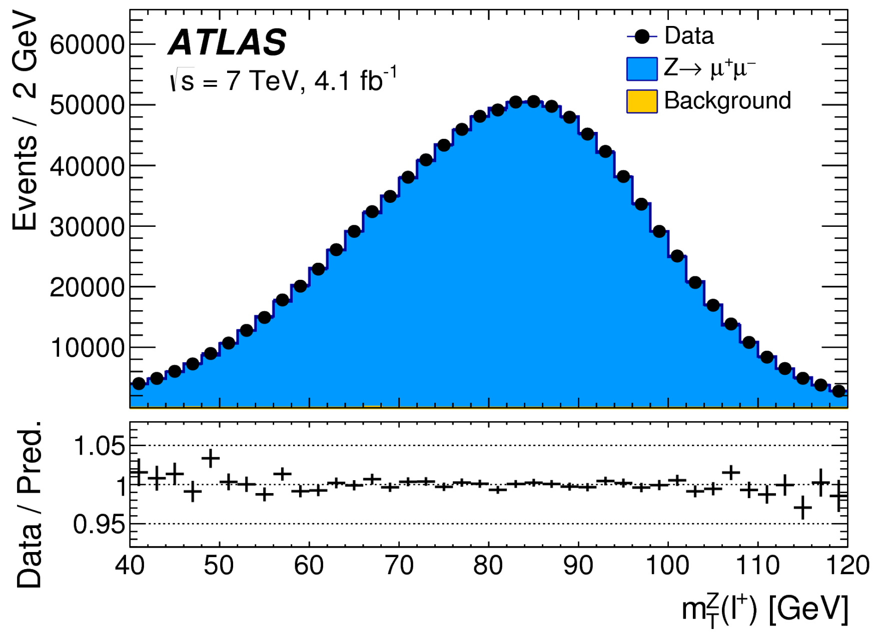

Cross checks with Z events

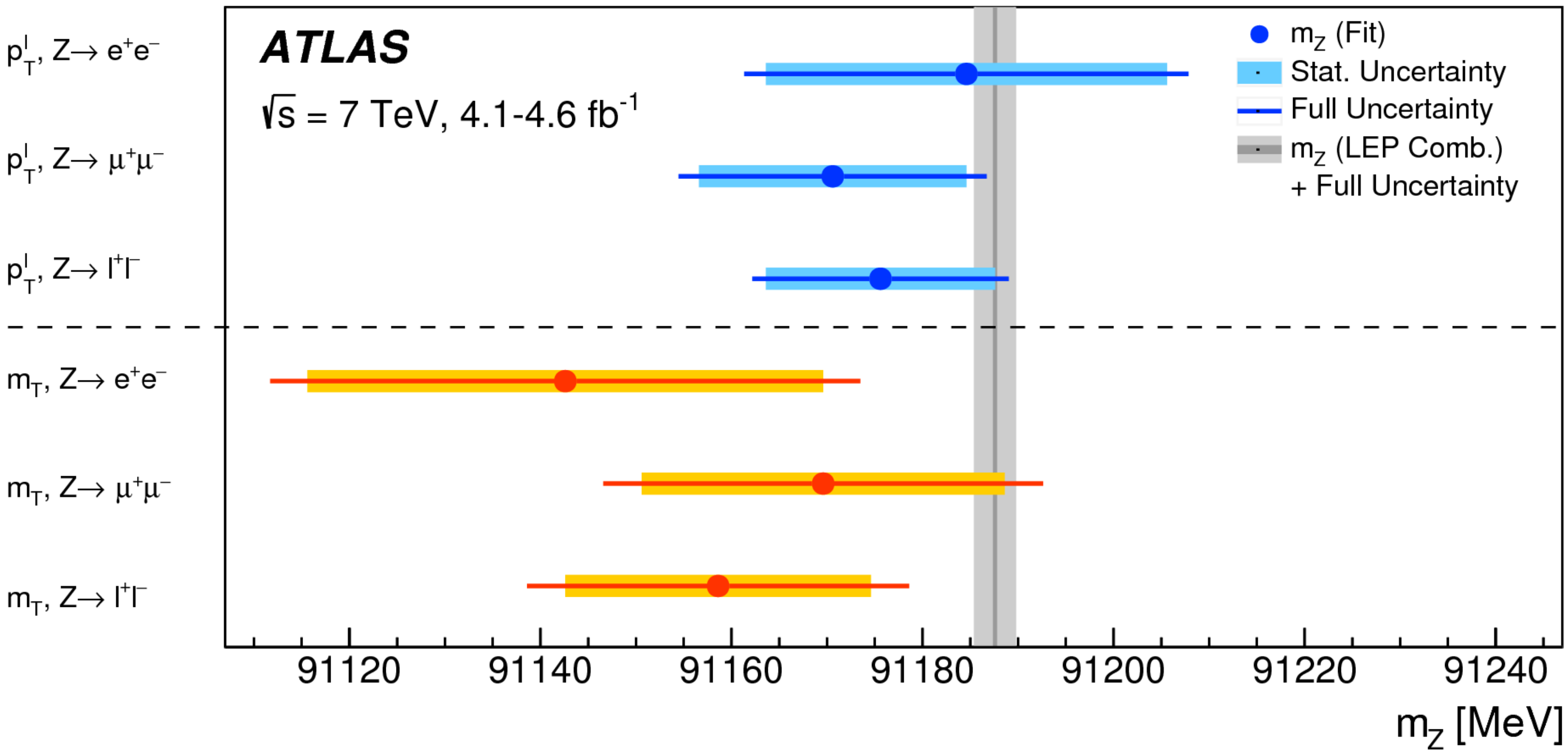

Lepton charge Distribution	ℓ^+ p_T^ℓ	ℓ^+ m_T	ℓ^- p_T^ℓ	ℓ^- m_T	Combined p_T^ℓ	Combined m_T
Δm_Z [MeV]						
$Z\to ee$	$13\pm31\pm10$	$-93\pm38\pm15$	$-20\pm31\pm10$	$4\pm38\pm15$	$-3\pm21\pm10$	$-45\pm27\pm15$
$Z\to\mu\mu$	$1\pm22\pm\ 8$	$-35\pm28\pm13$	$-36\pm22\pm\ 8$	$-1\pm27\pm13$	$-17\pm14\pm\ 8$	$-18\pm19\pm13$
Combined	$5\pm18\pm\ 6$	$-58\pm23\pm12$	$-31\pm18\pm\ 6$	$1\pm22\pm12$	$-12\pm12\pm\ 6$	$-29\pm16\pm12$

Results are consistent with the combined LEP value of m_Z
within experimental uncertainties

Backgrounds in W

Electroweak and top-quark backgrounds are determined from simulation

Multijet background is determined using data-driven techniques:

- define background-dominated fit regions with relaxed cuts of the event selection
- template fits in these regions to 3 observables: p_T^{miss}, m_T and p_T^l/m_T
- control regions are obtained by inverting the lepton isolation requirements

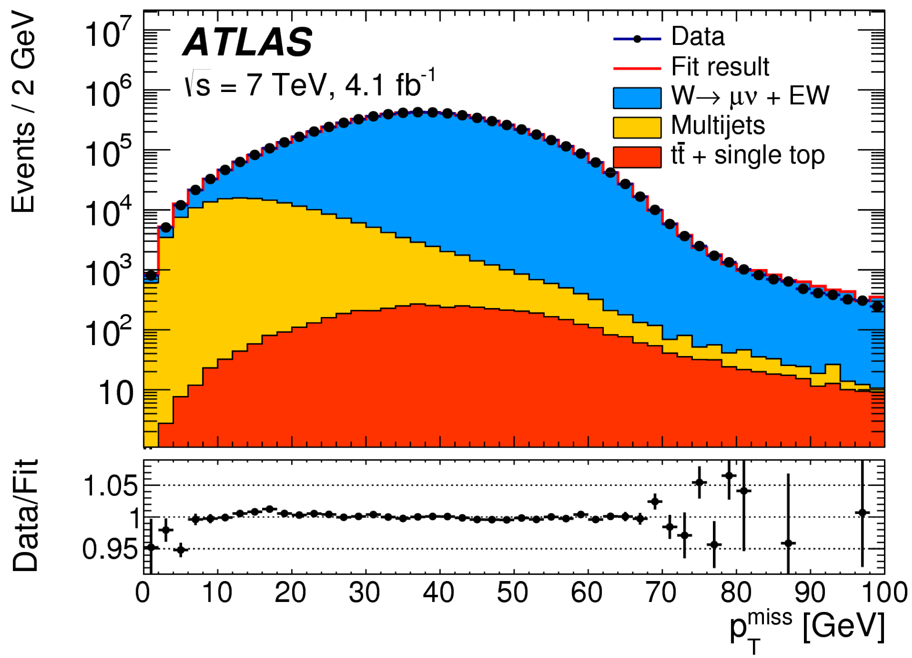

$W \to \mu\nu$						
Category	$W \to \tau\nu$	$Z \to \mu\mu$	$Z \to \tau\tau$	Top	Dibosons	Multijet
$W^\pm$ $0.0 < \lvert\eta\rvert < 0.8$	1.04	2.83	0.12	0.16	0.08	0.72
$W^\pm$ $0.8 < \lvert\eta\rvert < 1.4$	1.01	4.44	0.11	0.12	0.07	0.57
$W^\pm$ $1.4 < \lvert\eta\rvert < 2.0$	0.99	6.78	0.11	0.07	0.06	0.51
$W^\pm$ $2.0 < \lvert\eta\rvert < 2.4$	1.00	8.50	0.10	0.04	0.05	0.50
$W^\pm$ all η bins	1.01	5.41	0.11	0.10	0.06	0.58
W^+ all η bins	0.99	4.80	0.10	0.09	0.06	0.51
W^- all η bins	1.04	6.28	0.14	0.12	0.08	0.68
$W \to e\nu$						
Category	$W \to \tau\nu$	$Z \to ee$	$Z \to \tau\tau$	Top	Dibosons	Multijet
$W^\pm$ $0.0 < \lvert\eta\rvert < 0.6$	1.02	3.34	0.13	0.15	0.08	0.59
$W^\pm$ $0.6 < \lvert\eta\rvert < 1.2$	1.00	3.48	0.12	0.13	0.08	0.76
$W^\pm$ $1.8 < \lvert\eta\rvert < 2.4$	0.97	3.23	0.11	0.05	0.05	1.74
$W^\pm$ all η bins	1.00	3.37	0.12	0.12	0.07	1.00
W^+ all η bins	0.98	2.92	0.10	0.11	0.06	0.84
W^- all η bins	1.04	3.98	0.14	0.13	0.08	1.21

Kinematic distribution	p_T^ℓ				m_T			
Decay channel	$W \to e\nu$		$W \to \mu\nu$		$W \to e\nu$		$W \to \mu\nu$	
W-boson charge	W^+	W^-	W^+	W^-	W^+	W^-	W^+	W^-
δm_W [MeV]								
$W \to \tau\nu$ (fraction, shape)	0.1	0.1	0.1	0.2	0.1	0.2	0.1	0.3
$Z \to ee$ (fraction, shape)	3.3	4.8	–	–	4.3	6.4	–	–
$Z \to \mu\mu$ (fraction, shape)	–	–	3.5	4.5	–	–	4.3	5.2
$Z \to \tau\tau$ (fraction, shape)	0.1	0.1	0.1	0.2	0.1	0.2	0.1	0.3
WW, WZ, ZZ (fraction)	0.1	0.1	0.1	0.1	0.4	0.4	0.3	0.4
Top (fraction)	0.1	0.1	0.1	0.1	0.3	0.3	0.3	0.3
Multijet (fraction)	3.2	3.6	1.8	2.4	8.1	8.6	3.7	4.6
Multijet (shape)	3.8	3.1	1.6	1.5	8.6	8.0	2.5	2.4
Total	6.0	6.8	4.3	5.3	12.6	13.4	6.2	7.4

Summary of different corrections

After all corrections are applied, consistent results are achieved between different channels, observables, categories, charges and only after results were unblinded.

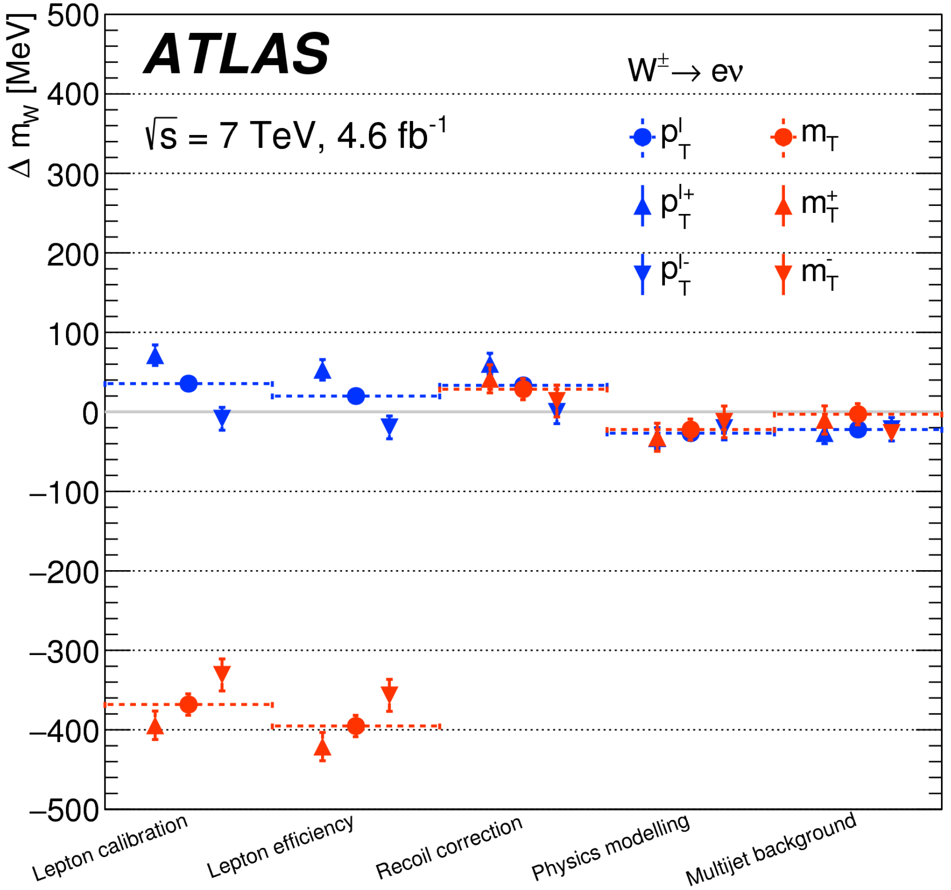

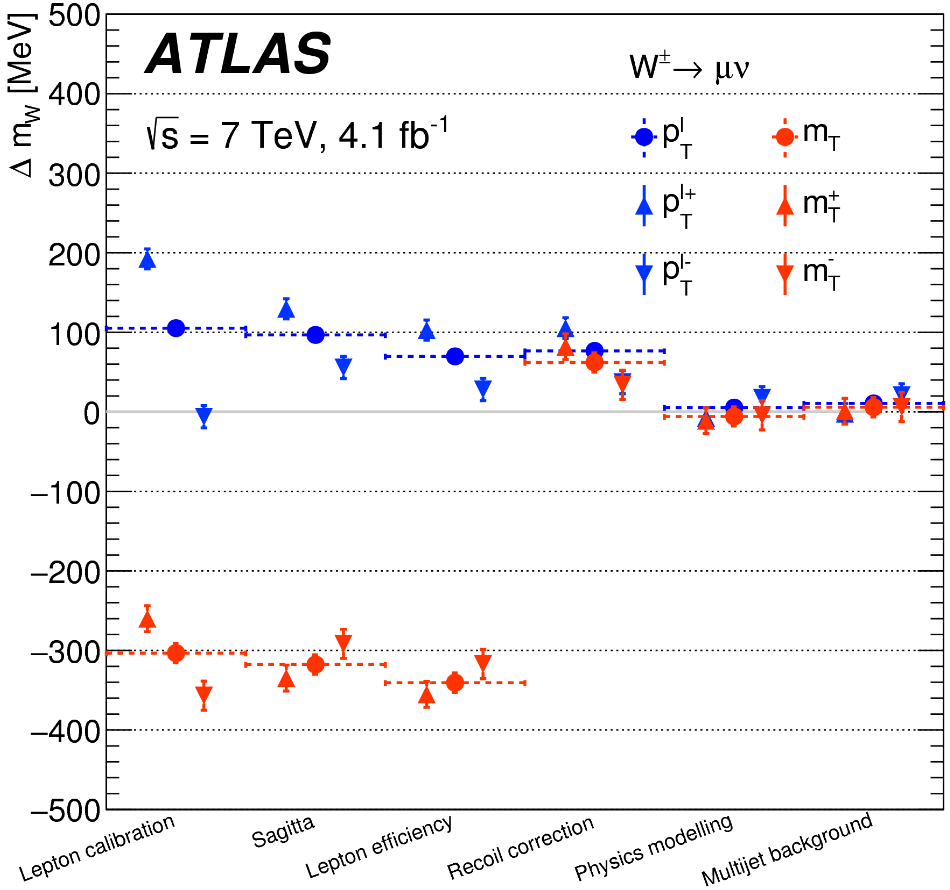

W control distributions: eta, pT

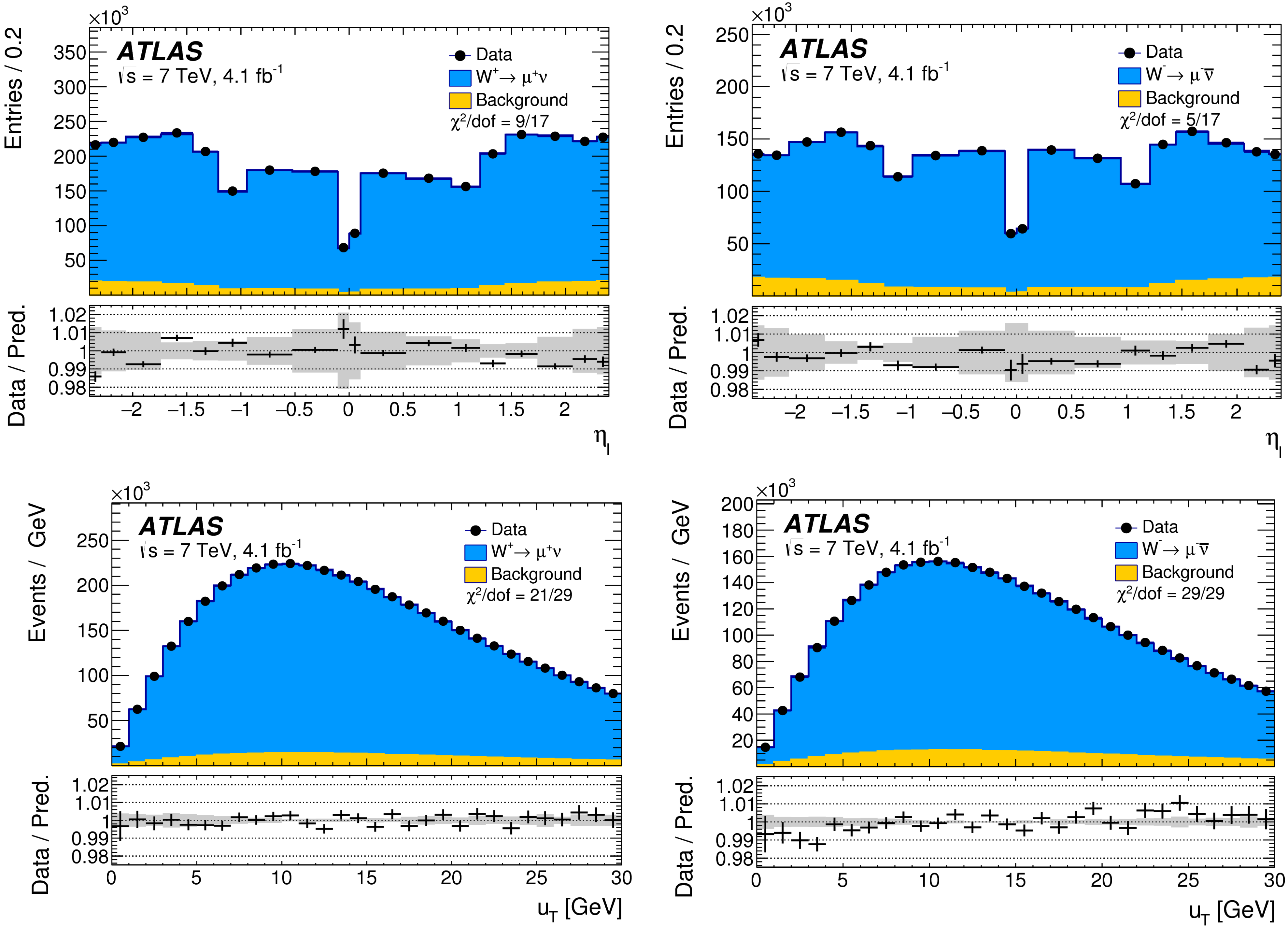

W mass-sensitive distributions: p_T^l and m_T

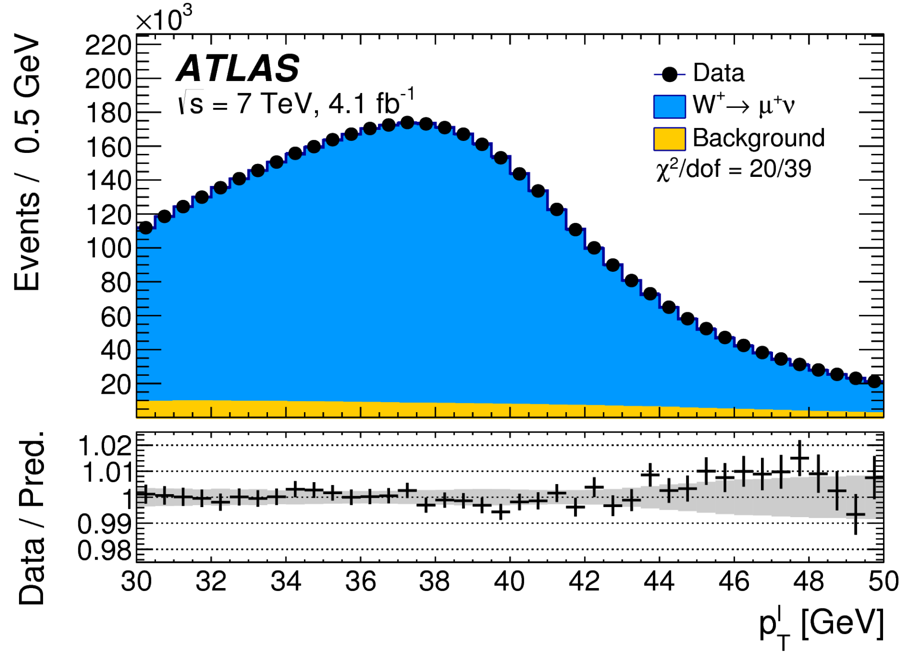

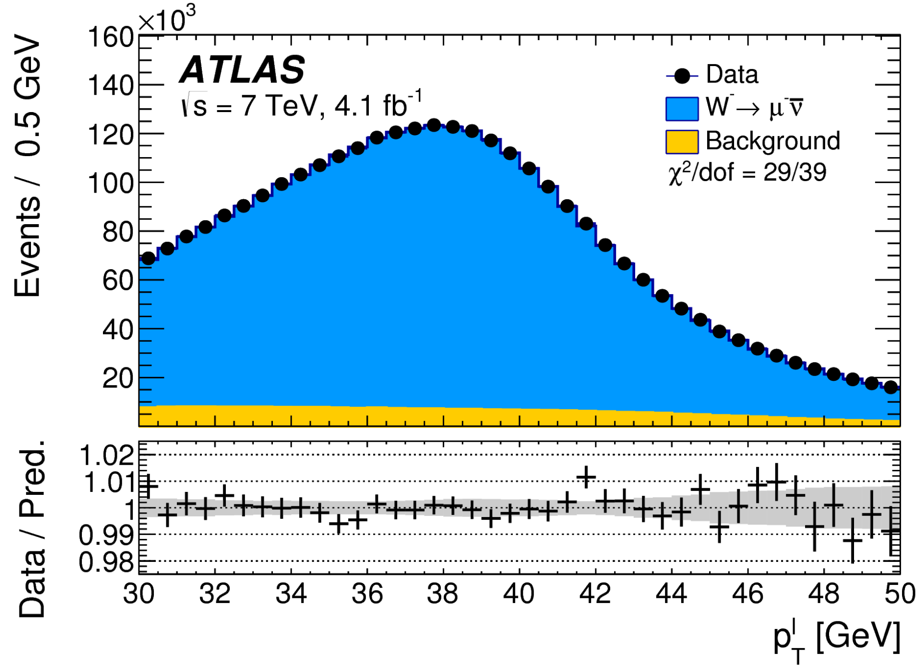

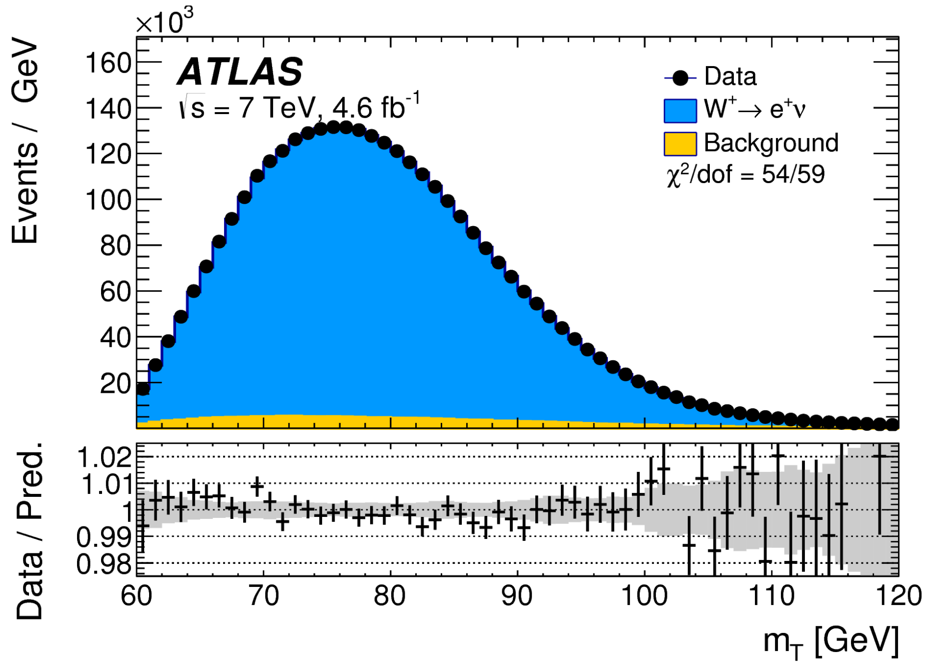

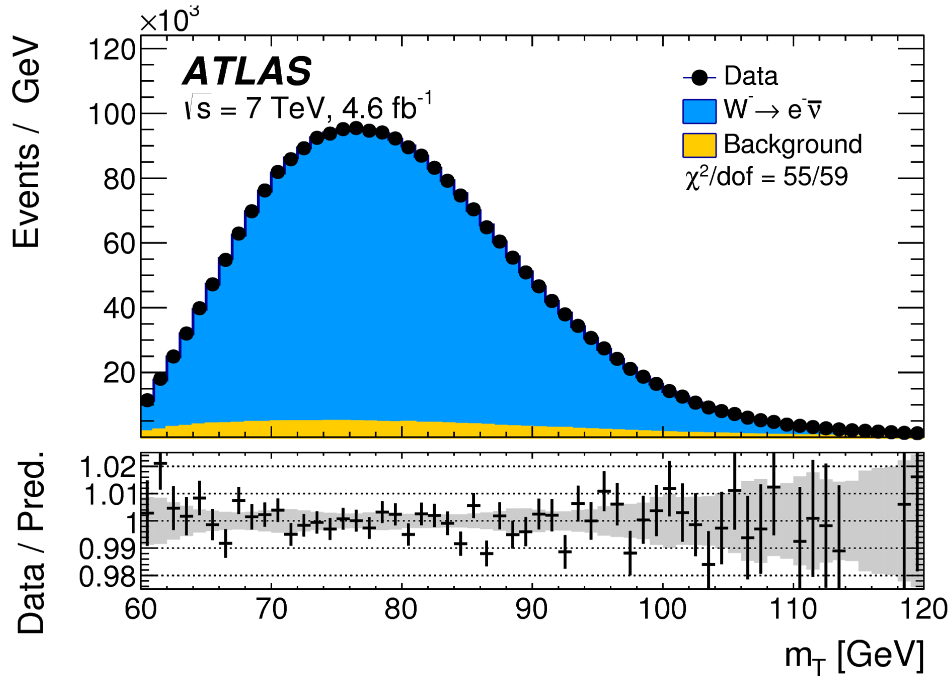

Consistency of the results

The consistency of the results was checked in the different categories but also in different pileup, u_T and $u_{//}$ bins

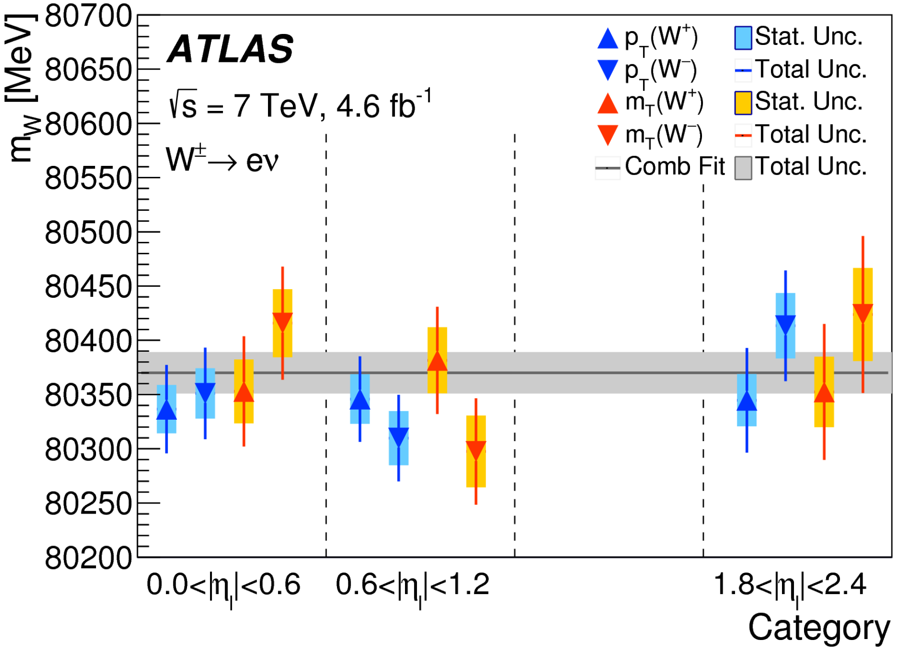

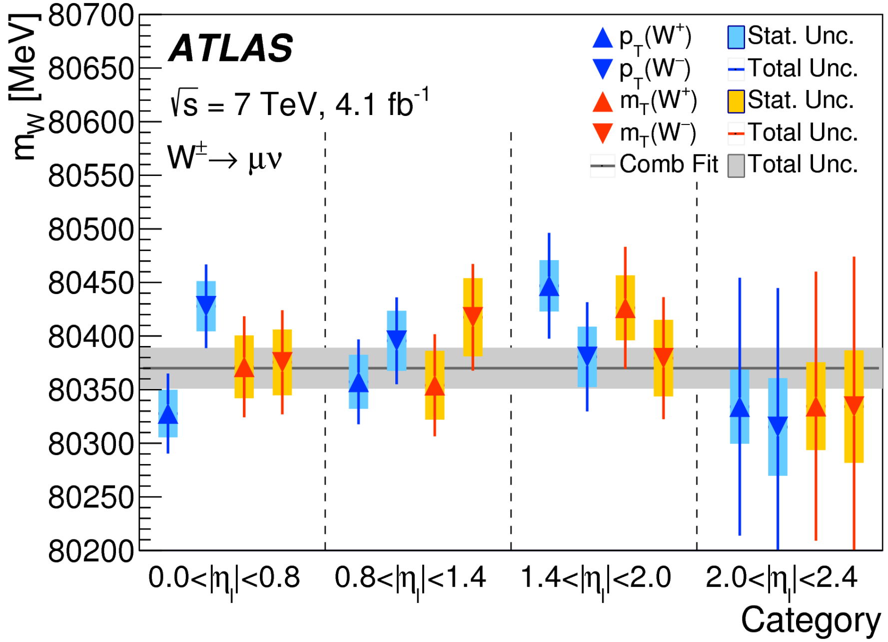

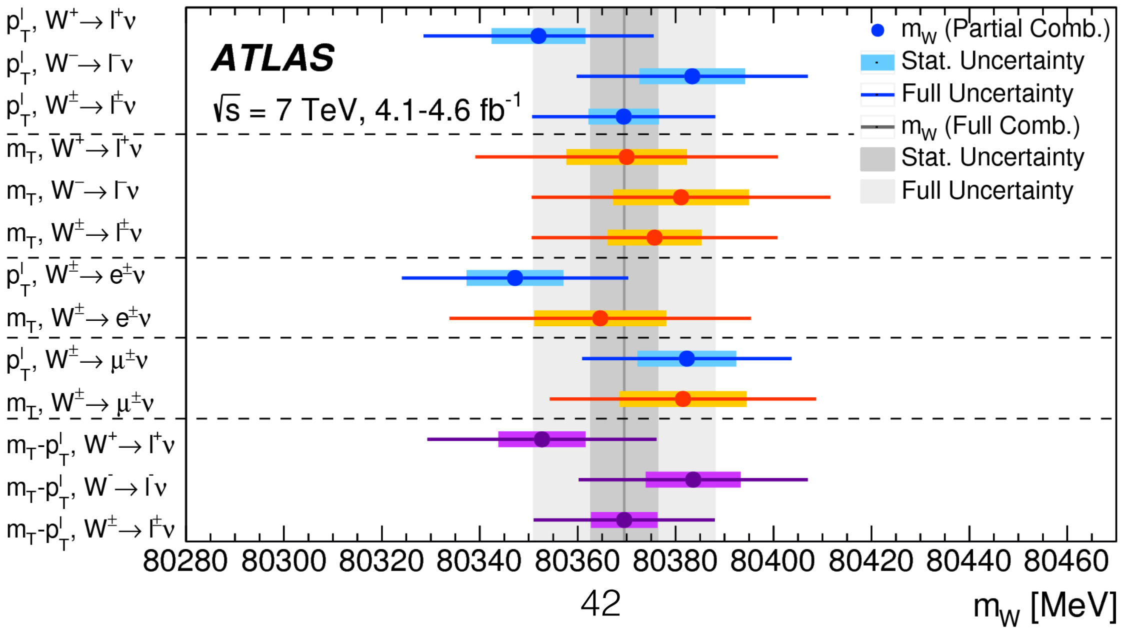

Results

$$m_W = 80369.5 \pm 6.8\ \text{MeV}(\text{stat.}) \pm 10.6\ \text{MeV}(\text{exp. syst.}) \pm 13.6\ \text{MeV}(\text{mod. syst.})$$
$$= 80369.5 \pm 18.5\ \text{MeV},$$

Combined categories	Value [MeV]	Stat. Unc.	Muon Unc.	Elec. Unc.	Recoil Unc.	Bckg. Unc.	QCD Unc.	EWK Unc.	PDF Unc.	Total Unc.	χ^2/dof of Comb.
m_T-p_T^ℓ, $W^\pm$, e-μ	80369.5	6.8	6.6	6.4	2.9	4.5	8.3	5.5	9.2	18.5	29/27

$$m_{W^+} - m_{W^-} = -29 \pm 28\ \text{MeV}$$

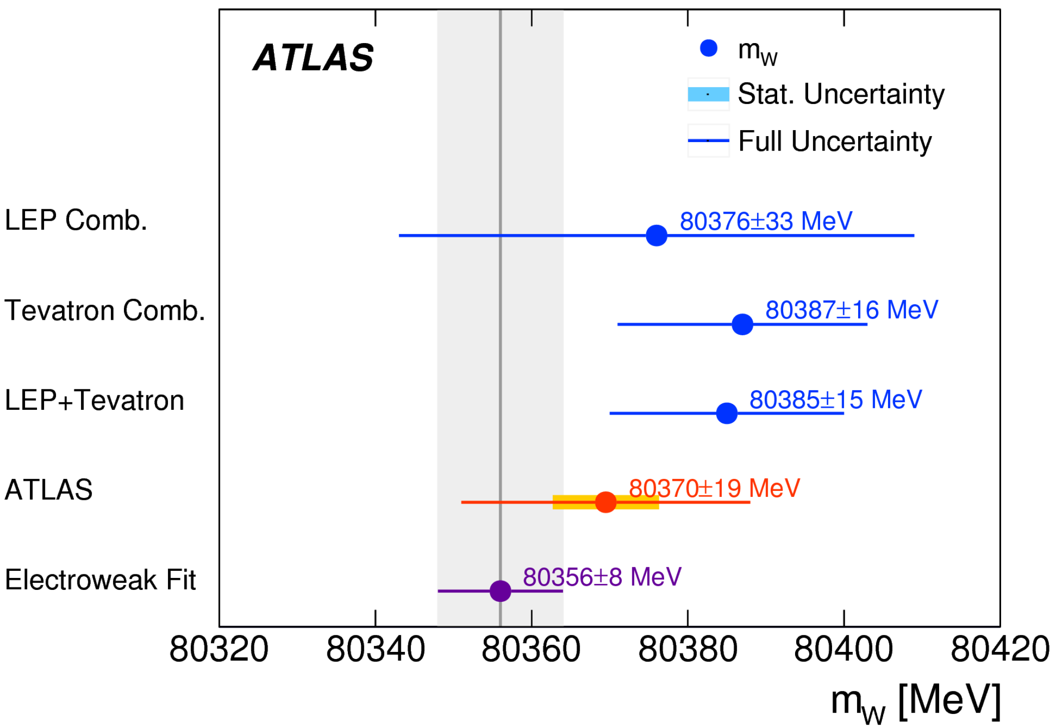

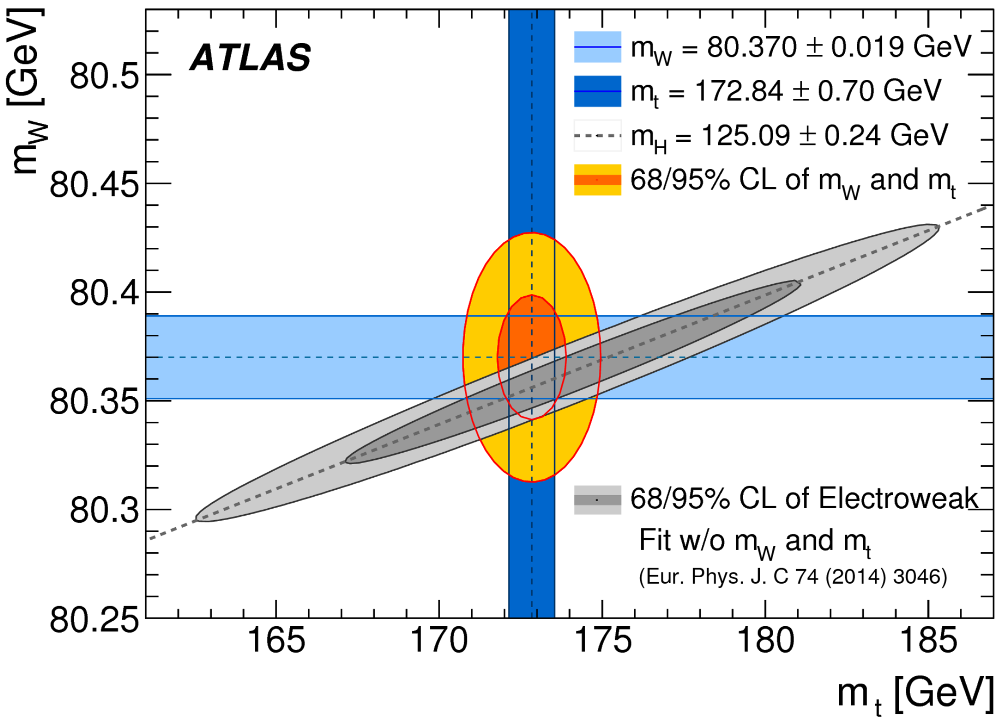

The result is consistent with the SM expectation, compatible with the world average and competitive in precision to the currently leading measurements by CDF and D0

Conclusion

The first LHC measurement of mW = 80370+/-19 MeV is public now arXiv: 1701.07240v1 after many years of effort in the ATLAS collaboration.

The central value is consistent with the SM prediction and with the current world average value.

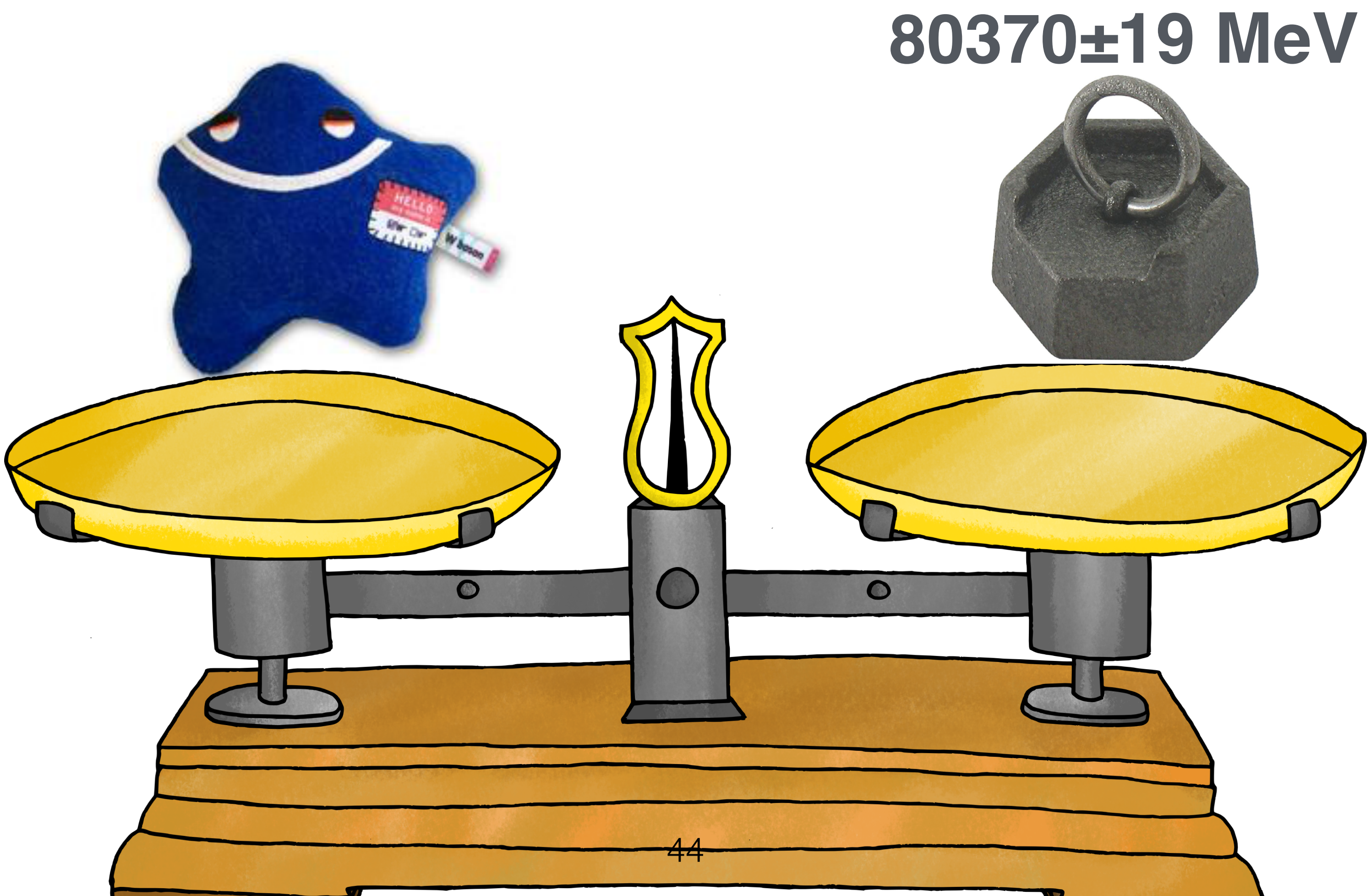

Perspectives

The uncertainty is dominated by theoretical modelling uncertainties, therefore more work in this direction is required and *a fully consistent model within one simulation tool* is needed

Not yet the same picture as for the 750 GeV excess :)

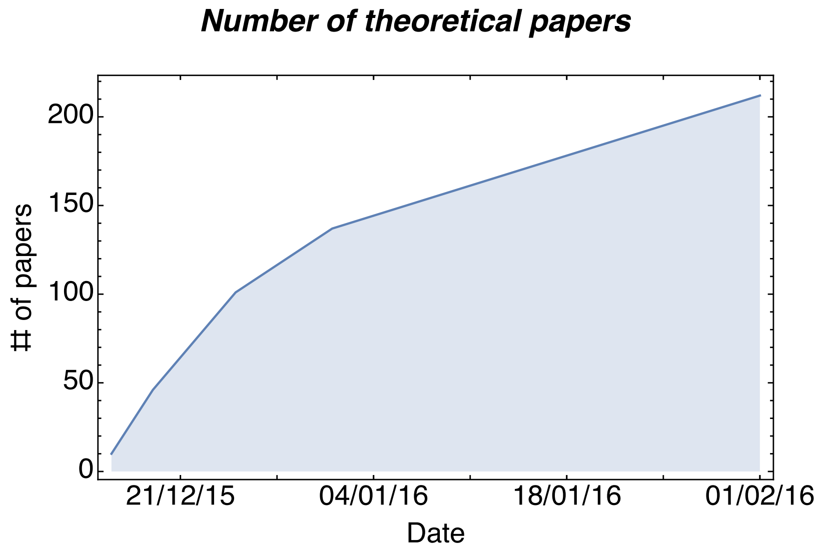

More data are available with the 8 and 13 TeV datasets which can be used to improve the analysis and to further constrain the PDFs. Experimentally, with the increase of the statistics in Z sample, most of the calibration uncertainties can be reduced. While more work is needed (already started) on the recoil with the increasing pileup.